Osteoarthritis modeling using a 3D in vitro osteochondral scaffold

Atur Patel

Tufts University

Biomedical Engineer 2011

Senior Honors Thesis

4/11

ACKNOWLEDGEMENTS

Special thanks to my mentors, Lin Sun and Rebecca Scholl-Hayden for assisting me with experimental design, answering my questions, and showing me how to use instrumentation I was unfamiliar with. Thanks to Leah Bellas for assisting me with histology. Finally, thanks to David Kaplan and Fiorenzo Omenetto for advising me throughout the project. All of these people along with the Tufts Biomedical Engineering Department were instrumental for the successful completion of this project.

TABLE OF CONTENTS

INDEX OF TABLES

INDEX OF FIGURES

1. Introduction.

Osteoarthritis is the most prevalent form of joint disease, affecting millions of people in the US. It is estimated that 80% of the population will have radiographic osteoarthritis by the age of 65, and of those 60% will develop symptoms [1]. Currently, most models for this common, yet complex disease have focused on animal studies [2]. Such models involve inducing osteoarthritis in animals and studying their joints for physical and biochemical changes. Some in vitro models have also been constructed. These models, however, involve using either limited, 2D monolayer cultures or simply extracting animal joints. None of the currently available models give the control, reproducibility, and physiological equivalence necessary for a successful model. The animal models lack control, are expensive, and have limited availability. The current in-vitro models are not much better. They are either physiologically irrelevant (2D models) or suffer from the same problems as animal models. The field is in need of a cheap model that can satisfy all of the necessary requirements. With a realistic and robust model, osteoarthritis research can be greatly accelerated and the lives of millions of people can be improved.

This study was conducted to provide a novel model system that will significantly improve the predictive power and realism of osteoarthritis models. The proposed system involves a 3D, in vitro, bone-cartilage coculture that can reasonably depict native joint structure. Osteoarthritis can then be induced and studied in a highly controllable, precise, and realistic way.

In this study, a potential in-vitro osteoarthritis model was successfully implemented and tested. The model consisted of a novel osteoblast scaffold embedded with chondrocyte alginate beads. Osteoarthritis was induced with the cytokines, IL-1β and TNF-α, which have been shown to play a significant role in osteoarthritis development [3, 4, 5, 6]. Testing concluded that the proposed model with some suggested modifications has potential in simulating osteoarthritis. However, further testing and design modifications are necessary before any conclusive statements can be made regarding the success of this model.

2. Background and Past Work

2.1. Osteoarthritis Pathology and Etiology

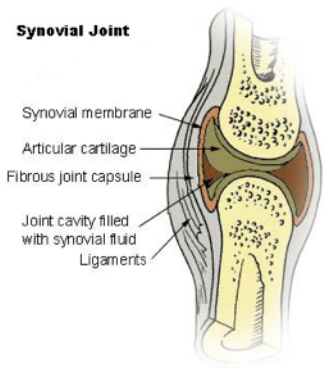

Figure 2.1 – A depiction of the synovial joint [7]

Osteoarthritis is a disease that can affect any synovial joint in the body but is most commonly seen in the hand, hip, and knee joints. In general, articular joints are composed of the epiphyseal end of a bone, articular cartilage, ligaments, and a capsule filled with lubricating synovial fluid (Figure 2.1) [7, 8]. Osteoarthritis results in the loss of hyaline cartilage, which in turn causes extensive remodeling of the adjacent bone. The remodeling results in the formation of bone outgrowths called osteophytes [1, 9, 10]. This remodeling effort is most likely an attempt by the body to compensate for the structural change caused by cartilage degradation. However, this compensation mechanism is not perfectly effective and often leads to symptomatic osteoarthritis, which leads to pain and inflammation [1]. Osteoarthritis is commonly perceived as a "wear and tear" disease. However, studies have shown that cartilage from osteoarthritis joints has decreased proteoglycan content and differs from healthy tissue biochemically, indicating that at least some aspect of the disease is not linked to wear and tear [11]. Furthermore, these components of the pathology indicate that both cartilage and bone are very important aspects of the disease.

On a cellular level, osteoarthritis is characterized by a disturbance in the normal balance of anabolism and catabolism typically seen in articular cartilage chondrocytes [12]. This disturbance leads to increased levels of certain metalloproteinases (MMPs) and aggrecanases (ADAMTS) that in turn cause cartilage degradation. Furthermore, during osteoarthritis development, certain anabolic pathways are also activated resulting in the formation of aberrant types of collagen (type X, III, and VI) [12, 13]. This further leads to a structural change in the collagen matrix, which may cause the symptoms associated with osteoarthritis.

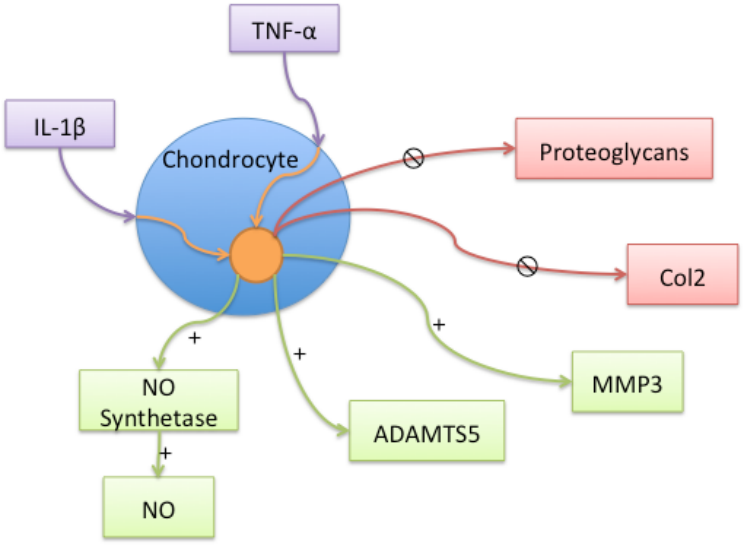

Figure 2.2 – Summary of the effects of IL-1β and TNF-α on osteoarthritic chondrocytes. Green arrows with + symbols represent up-regulation and red arrows with ⊘ symbols represent down-regulation.

Many of these catabolic and anabolic changes are associated with proinflammatory cytokines. Specifically, TNF-α and IL-1β have been heavily implicated in osteoarthritis development [14]. It's been established that IL-1β is capable of promoting the release of nearly every proteinase involved in osteoarthritic cartilage degradation [12, 15]. Furthermore, IL-1β inhibits the synthesis of proteoglycans like aggrecan and Type II collagen and promotes the synthesis of nitric oxide via nitric oxide synthetase, which can further enhance proteinase production (Figure 2.2 and Figure 2.4) [16, 17]. Nitric Oxide acts an autocrine to reduce aggrecan synthesis and stimulate MMP activity. It has been found in increased quantities in the synovial fluid of osteoarthritis patients [18, 12, 16]. Some studies suggest that IL-1β is synthesized by chondrocytes and acts as an autocrine or paracrine. TNF-α has been shown to have similar effects to IL-1β though with reduced potency [12, 15, 6, 14]. Because of these widespread osteoarthritic effects, TNF-α and IL-1β have successfully been used to induce osteoarthritis in previous in vitro and in vivo models [3].

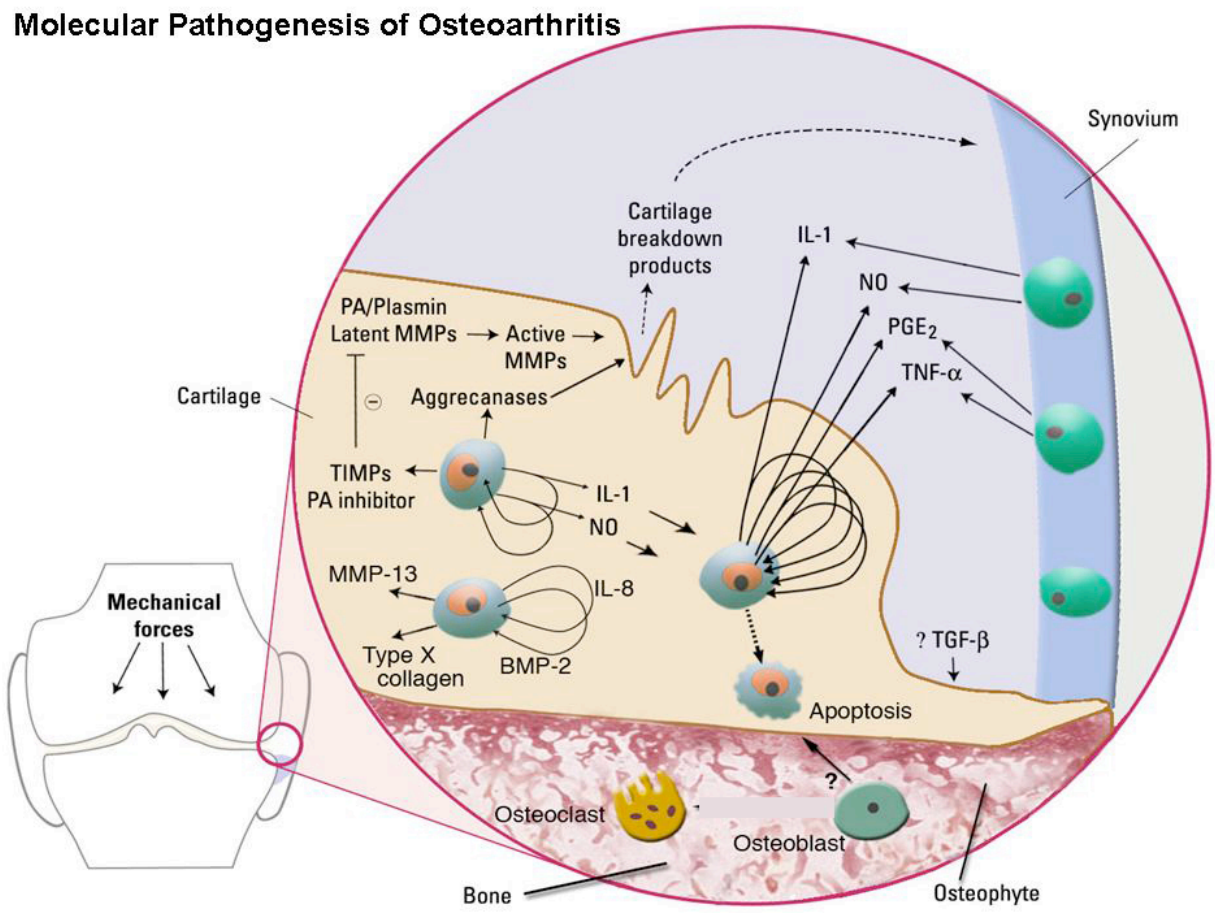

Figure 2.3 – Broad overview showing some potential pathways involved in the molecular pathogenesis of osteoarthritis [19]

Another proposed component of the pathogenesis of osteoarthritis is the apoptotic death of chondrocytes [13, 19]. This may explain the hypocellularity commonly seen in osteoarthritis. Upregulation of caspases by various mediators such as TNF-α and nitric oxide may contribute to this aberrant apoptosis [13, 16, 20].

The role that bone plays in osteoarthritis is not as well characterized as cartilage. In fact, therapies considering both bone and cartilage have only recently been investigated [9]. There is increasing evidence that the relationship between subchondral bone and articular cartilage plays an important role in osteoarthritis development. Notable changes in the subchondral bone of osteoarthritis patients include: increased turnover, sclerosis, osteophyte formation, thinning, and reduction in elasticity [9]. The interface between subchondral bone and articular

cartilage is simply a layer of calcified cartilage indicating the likeliness of bone-cartilage intercommunication [9, 21, 10].

While the pathology of osteoarthritis after its development is more or less understood, its underlying etiology is still mostly unknown. A wide range of risk factors is present for this complex disorder. It is more prevalent with increased age, obesity, with previous injury and with high bone density, but there are also genetic factors involved. It is important to note that while there is a correlation between joint wear and tear (due to athleticism and age) this is not necessarily the cause of the disorder as demonstrated by many cases of athletes and elderly who have not developed the condition [1].

2.2. Past Studies – Animal Models

In an effort to shed more light on this complex, multifaceted disorder scientists have built models to study the disease. Most commonly, murine and canine animal models are used [22]. Such models work well to show some of the long-term effects of the disease and give scientists a way to study the disease in living systems without harming humans. However, there are many limitations to these models. Every animal that is used is different in some way and thus many uncontrollable variables are introduced into the experimental system. This variability has led to the development of many models and no universal gold standard exists [22]. This makes it far more difficult to get accurate, reproducible results and much harder to interpret the results of other researchers.

Another limitation is the lack of reliability inherent in most interspecies comparisons. The results obtained from animal systems may not necessarily apply to humans. Many important anatomical and physiological differences exist between humans and animals so things learned from animal models cannot always be extrapolated to humans.

Furthermore, animal models are costly, inefficient and limited in availability. Some of the more elaborate and realistic animal models require special facilities for breeding and studying

animals. This limits the number of available animal models, accessibility to researchers, and efficiency. Additionally, the cost of the animals, facilities and specialized personnel make these models far more expensive.

Finally, an often overlooked but important issue to consider is the ethical aspect of animal research. Animal research is subject to controversy, especially when the animals are sacrificed or subjected to pain.

2.3. Past Studies – In Vitro Models

Many of the issues mentioned with animal models can be resolved with in vitro models. However, due to the difficulty in producing accurate in vitro models, animal models are far more popular. The few studies that have been conducted have focused only on one tissue type or one part of the complex joint system. For instance, one study explored an in vitro model using chondrocytes from infected horse joints. In this study the cartilage was subjected to a single-impact load and the resulting effects on the cartilage were monitored [23]. Similarly, another study used 2D slices of human osteoarthritic cartilage to model osteoarthritis metabolic activity. Again, only cartilage was studied [24]. While these studies were successful in that the observed cartilage degradation patterns were similar to that of osteoarthritis, they neglected to include bone, a key component to the osteoarthritis system [9, 21, 10]. Furthermore, these models and most other in vitro models have used 2D systems, which grossly impacts their predictive power. Joints are 3-dimensional, highly structured constructs and modeling them with a 2D system is inaccurate. Other studies have tried making in-vitro models by extracting entire osteoarthritic joints from animals [25]. Such studies are only marginal improvements over animal studies as they still suffer from many of the same issues and offer only slightly more control.

2.4. An Improved Model

If in vitro models are to succeed and offer an alternative to animal models they must offer a more thorough and robust model of the disease. No in vitro, osteoarthritis models have been

developed that incorporate every relevant part of the system, that is: osteoblasts, chondrocytes, and a 3D matrix. While, the structure of joints is far more complex and includes many more components, a system with just these parts would greatly improve the current state of the art. If such a model could be created, research in the field of osteoarthritis could greatly be accelerated. This would provide researchers with a fully controllable, reliable, and flexible system.

Certain aspects of this improved model have been shown to be possible in past studies. One key feature necessary for this modeling system is an osteochondral coculture. As mentioned previously, the pathology of osteoarthritis not only involves cartilage degradation but also a complex bone remodeling response. In fact, it is the response of the bone to cartilage degradation that often leads to many of the symptoms that patients may experience. Past studies have shown successful cocultures of osteocytes and chondrocytes on polycaprolactone 3D scaffolds by culturing each half of the scaffolds separately (Figure 2.4) [26]. The issue with methods such as these is that only a single 2-dimensional osteochondral interface is formed which is harder to study and isn't as accurate. However, this study does demonstrate that the proposed tissue engineering based model is possible with current biomedical technologies. The proposed model, unlike this study, optimizes the osteochondral coculture by establishing a design that emphasizes the osteochondral interface and goes one step further by using this 3D system to model osteoarthritis. This model includes a simple but effective way to induce osteoarthritis on an in vitro system. With proper refinement and testing a robust model of osteoarthritis should be relatively easy to develop.

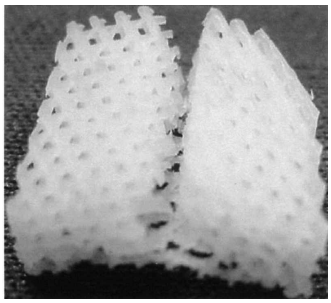

Figure 2.4 – Split polycaprolactone scaffolds with osteocytes cultured on one side and chondrocytes on the other [26].

Once developed, this system will significantly improve the capacity to research osteoarthritis. The proposed model system is superior to existing in vitro models and can either complement or replace animal studies. The large quantity of affected osteoarthritis patients and the relative

gap in understanding of the disease make it especially important to develop an accurate, realistic, and highly controllable model system. In the long run this will facilitate the production of therapeutic medications and preventative measures against osteoarthritis, which can potentially improve the lives of millions of osteoarthritis patients.

3. Experimental Design

3.1. Specific Aims

The long-term goal of this study is to make an in vitro model for osteoarthritis that will be realistic, cheap, and highly controllable. The immediate objective of this study is the development of a 3D system that can be induced to resemble osteoarthritis. The successful development of such a system is an important first step to this goal. The central hypothesis was that this system would physiologically, chemically, and structurally mimic the joint system so that eventually it can be used to model joint diseases, in particular, osteoarthritis. This hypothesis aimed to test the physiological realism of the system that was created in this study. The rationale for this study was to establish a model system to facilitate the study of osteoarthritis.

To achieve the objectives outlined in this study the following specific aims were attempted:

Aim 1: Develop an osteochondral coculture system that can easily be manipulated and studied to facilitate osteoarthritis modeling. The working hypothesis was that by separately culturing osteoblast and chondrocyte scaffolds and combining them in a particular way, a coculture system could be made. The outcome for this aim was a 3D co-culture of osteoblasts and chondrocytes mimicking native joints.

Aim 2: Assess the effects of specific cytokines on the induction of osteoarthritis like symptoms on a 3D osteochondral scaffold. The working hypothesis was that osteoarthritis could be induced in vitro by exposing the coculture system to specific cytokines. The outcome of this aim was an easy way to induce osteoarthritis in an in vitro system so that ultimately it can be modeled.

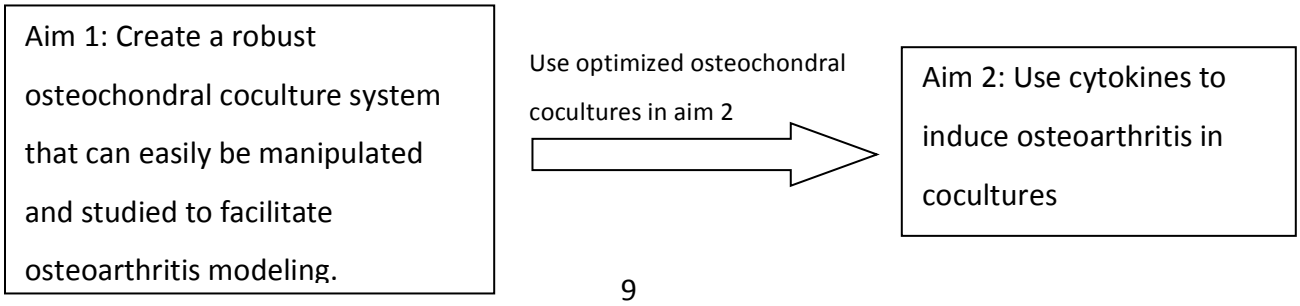

Figure 3.1 - Summary of aims

3.2. Experimental Setup and Summary

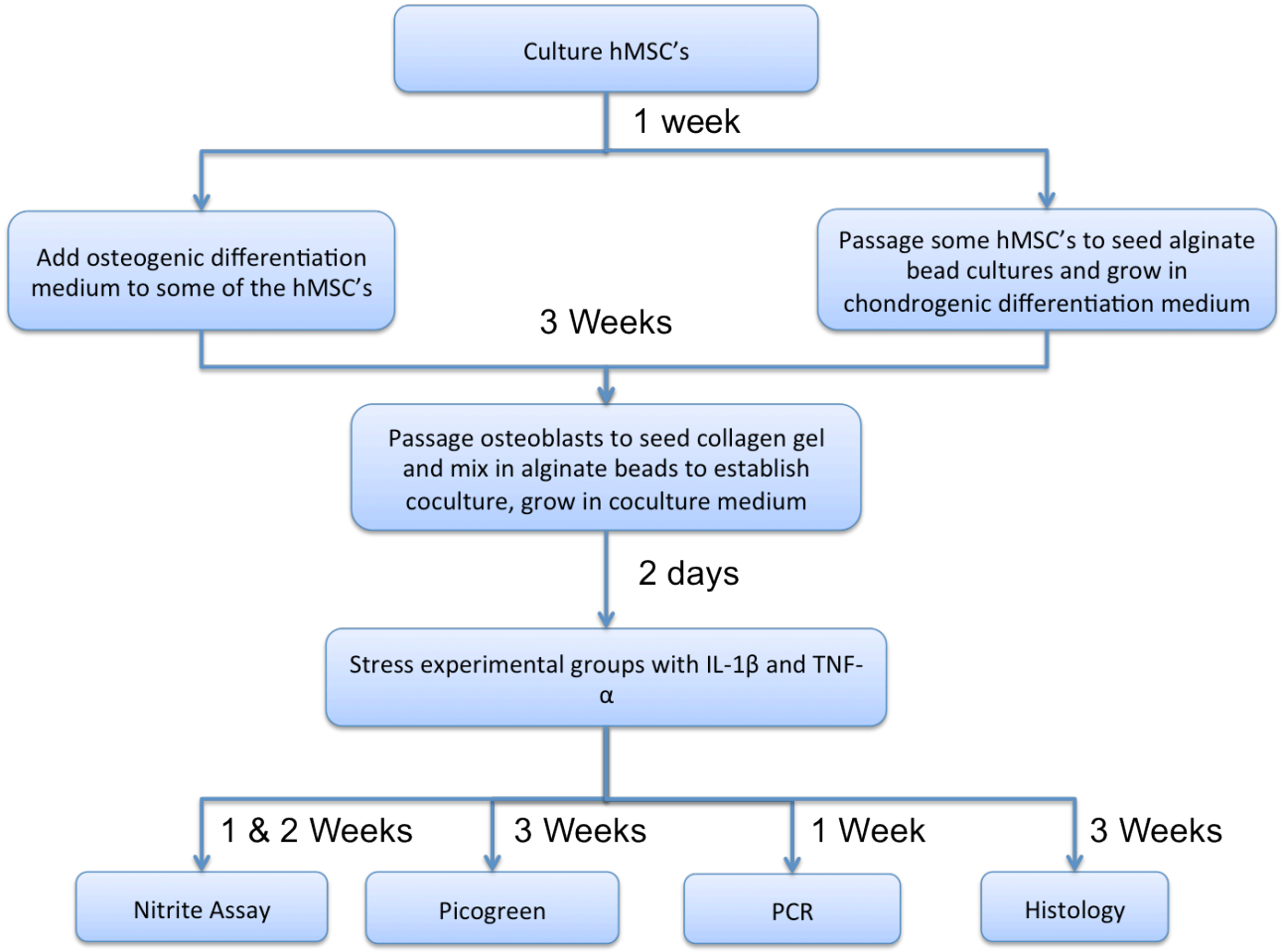

Figure 3.2 – Overview of the experiment, outlining all the steps used to achieve aims

Table 3.1 – Coculture (Aim 1) Experimental and Control Groups

Groups	**Purpose**	**Abbreviation**
Osteochondral coculture in coculture medium	Experimental Group	Coculture
Chondrocytes in coculture medium	Control Group	Chondrocytes
Osteoblasts in coculture medium	Control Group	Osteoblasts

Table 3.2 – Osteoarthritis Induction (Aim 2) Experimental and Control Groups

Groups	**Purpose**	**Abbreviation**
IL-1 β stimulation (50 pg/mL) of osteochondral coculture in coculture medium	Experimental group	IL-1 β
TNF-α stimulation (50 pg/mL) of osteochondral coculture in coculture medium	Experimental Group	TNF-α
Osteochondral coculture in coculture medium	Control Group	Coculture

As shown in Figure 3.2, this study involved growing human mesenchymal stem cells (hMSCs), differentiating them into osteoblasts and chondrocyte beads, and combining the two cell types to form an osteochondral collagen scaffold. The experimental groups (see Table 3.2) were stressed with the proinflammatory cytokines, IL-1β and TNF-α. To check the success of the aims, PCR, a nitrite assay, PicoGreen, and histology were performed. Table 3.1 and Table 3.2 show the experimental and control groups made to establish each aim. Note that the osteochondral coculture is an experimental group for one aim and a control group for the other.

3.3. Overview of Osteochondral Scaffold Design

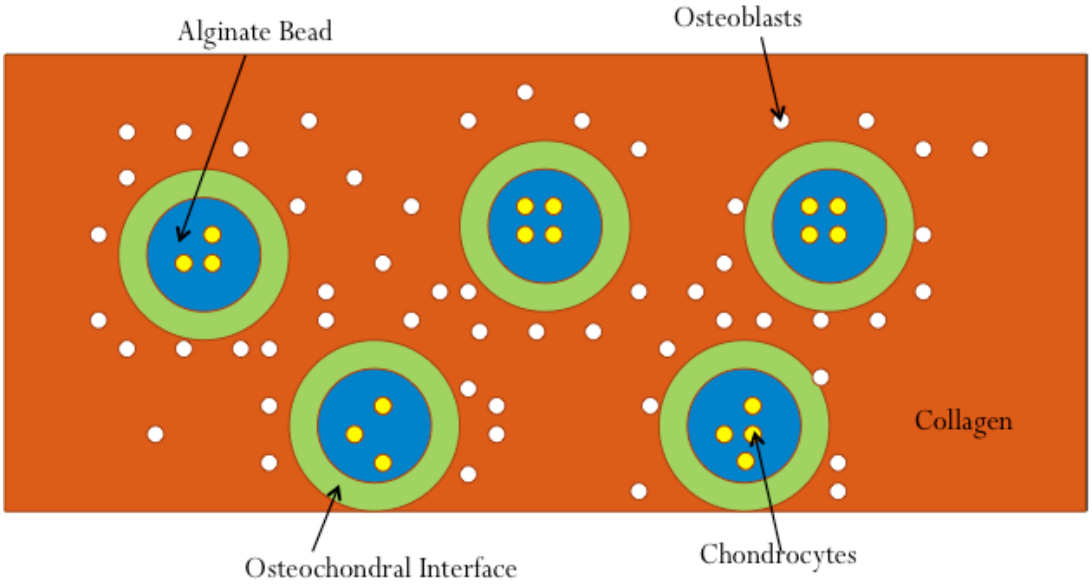

Figure 3.3 – Osteochondral scaffold design

The osteochondral coculture scaffold was designed to facilitate osteoarthritis research while still maintaining realism and physiological relevance. As shown in Figure 3.3, a collagen matrix seeded with osteoblasts was embedded with chondrogenic alginate beads. This system was thought to closely simulate in vivo conditions, especially regarding the interface between osteocytes and chondrocytes. Only a layer of calcified cartilage separates osteocytes and chondrocytes in native joints and this system closely mimics this [16]. The system includes a 3D matrix with both osteoblasts and chondrocytes, all of the relevant cell types in osteoarthritis.

Furthermore, this system improves upon previous coculture methods by establishing numerous osteochondral interfaces (between each bead and the surrounding collagen matrix) facilitating testing and studying of the system. To further enhance studying of this system, both the alginate beads and the surrounding collagen matrix can be digested with sodium citrate and collagenase, respectively [27, 28]. This makes it possible, in theory, to first digest the surrounding collagen matrix with collagenase and then isolate the beads and dissolve them in sodium citrate. Testing can then be performed on the alginate beads and the collagen matrix separately to study the effects of treatments on each cell type individually. This will give

researchers much more data when studying osteoarthritis with this model. This method of studying each cell type separately was not, however, applied in this study because of structural concerns and smaller than expected scaffolds as highlighted below in section 6.1.

3.4. Biomaterial Choice

Collagen type 1 (Col I) and alginate were chosen as biomaterials because they are natural polymers found natively in humans. Col I is a major component of the ECM of natural bone making it extremely suitable for this application [29]. Furthermore, type 1 collagen matrices have been shown to promote osteogenic differentiation, growth, adherence, and mineralization in numerous studies [29, 30, 31, 32]. Alginate beads have been shown to not only support chondrocyte growth but also maintain the chondrocyte phenotype for prolonged periods of time (up to 8 months) and re-differentiate chondrocytes that have dedifferentiated [33]. The alginate encapsulation also allows chondrocytes to respond to growth factors and cytokines so osteoblast-chondrocyte signaling can occur [33]. Furthermore, previous studies have shown that alginate beads support the differentiation of human mesenchymal stem cells (hMSC's) to chondrocytes and that by 18-24 days of culture the gene profiles of these hMSC derived chondrocytes are analogous to human articular cartilage [34].

These biomaterials are also very easy to dissolve or digest. Col I can easily be enzymatically digested with the protease, Collagenase Type 1 [27], facilitating the isolation of alginate beads so that the collagen and alginate components of this system can be studied and tested separately. Alginate readily dissolves in sodium citrate solution to free cells from the matrix making it easy to study cells embedded in alginate [28].

3.5. Cell sources

Osteoblasts and chondrocytes were differentiated from human mesenchymal stem cells (hMSC's) in this study. hMSC's were chosen because they are readily available, proliferative, and relatively cheap. They are multipotent and capable of differentiating into either

chondrocytes or osteoblasts [35]. Alternative cell sources, including native chondrocytes and osteoblasts are much harder to obtain, more expensive, and not as proliferative.

3.6. Osteoarthritis Induction

The cytokines, IL-1β and TNF-α were chosen to induce osteoarthritis on osteochondral cocultures in this study. These cytokines have been the best characterized in terms of their role in osteoarthritis [12, 15]. They have also shown the most promise in osteoarthritis induction in previous studies involving chondrocytes [3].

Other methods of inducing osteoarthritis were considered, including mechanical stress and macrophage stimulation. However, due to time constraints, these factors were not included in this study.

3.7. Tests and assays

RT-PCR was used to quantify gene expression in order to determine if osteoarthritis was successfully induced and to verify osteogenic and chondrogenic differentiation in the cocultures. The following genes were analyzed: ACAN, ADAMTS5, CASP3, MMP3, COL2A1, RUNX2, and SOX9.

The ACAN gene is responsible for aggrecan synthesis, which has been shown to be down-regulated in osteoarthritic tissue [5]. It can also indicate the presence of chondrocytes [36]. The ADAMTS5 gene encodes an aggrecanase enzyme that has been shown to be one of the most up-regulated aggrecanases in osteoarthritic tissue [37, 38]. The MMP3 gene encodes the matrix metalloproteinase-3 enzyme, which is responsible for digesting ECM proteins and has been shown to be one of the most up-regulated proteases during osteoarthritis [37]. The CASP3 gene encodes the caspase-3 enzyme, which is implicated in apoptotic pathways and thus up-regulated during osteoarthritis [20]. The COL2A1 gene encodes a component of type II collagen and a chondrocyte marker [36]. Type 2 collagen synthesis has been shown to be suppressed in osteoarthritic tissue [3]. The RUNX2 gene encodes a transcription factor responsible for osteoblast differentiation and was used as an osteoblast marker [39, 40, 41]. It

could also indicate bone remodeling [41]. The SOX9 gene encodes a transcription factor responsible for chondrocyte differentiation and was used as a chondrocyte marker [42].

In addition to PCR, nitrite levels were assessed with a Griess reagent Nitrite assay. Nitric oxide has been implicated in the osteoarthritis pathogenesis as an autocrine that reduces aggrecan synthesis and stimulates MMP activity [12, 16] and thus nitrite levels should be elevated in the osteoarthritis induced experimental groups.

Finally, PicoGreen analysis was conducted to quantify DNA levels in samples 3 weeks after culture. Hypocellularity, possibly due to apoptotic death, is a symptom of osteoarthritis [13] so a reduction in DNA levels should be seen in osteoarthritis induced experimental groups. Furthermore, PicoGreen was used to grossly determine cell quantities after prolonged culture.

4. Materials and Methods

4.1. hMSC Culturing and Expansion

Bone marrow derived hMSC's were cultured as 2 dimensional monolayers in T-185 tissue culture flasks in expansion medium (88% DMEM w/ high glucose and L-glutamine, 1% Non-essential amino-acids, 1% Pen-Strep-Fungizone, 10% FBS, 1 ng/mL bFGF). Medium was changed every 2-3 days and cultures were passaged upon 80% confluency until enough cells were present for differentiation.

4.2. Osteoblast Differentiation

After p3 hMSC's were about 80% confluent, hMSC expansion medium was replaced with osteogenic medium (88% DMEM w/ high glucose and L-glutamine, 1% Non-essential amino-acids, 1% Pen-Strep-Fungizone, 10% FBS, 100 nm dexamethasone, 10 mM β Glycerol Phosphate, 0.05 mM ascorbic acid [43]) to promote osteogenic differentiation. Cells were grown under these conditions for 3 weeks to ensure fully differentiated osteoblasts.

4.3. Chondrocyte Alginate Bead Construction and Differentiation

Alginate beads were constructed and seeded following the protocol provided with the Lonza alginate solution [44]. P3 hMSC's grown in T-185 tissue culture flasks were trypsinized and counted with a hemocytometer. Trypsinized cells were then centrifuged at 1250 RPM for 10 minutes to isolate a cell pellet. The pellet (≈$4.4*10^6$ cells) was washed once with 155 mM NaCl and was resuspended in 11 mL of 1.2% sodium alginate making an alginate solution with approximately $4*10^5$ cells/mL. The cell/alginate solution was then expressed dropwise through a 22 gauge needle into 4 volumes (≈45 mL) of 102 mM $CaCl_2$ solution to form beads. The $CaCl_2$ solution was removed and the beads were washed 5 times with 4 volumes (≈45 mL) of 155 mM NaCl. Finally, the beads were divided evenly into 24 well plates (3-4 beads per well) to produce 36 samples (9 samples per chondrocyte containing group outlined in Table 3.1 and Table 3.2) each with approximately $1.2*10^5$ cells ($4.4*10^6$ cells total ÷ 36 wells). The beads were grown in chondrogenic medium (95% DMEM with high glucose and L-glutamine, 1% Non essential

amino-acids, 2% FBS, 1% Pen-Strep-Fungizone, 1% Insulin – Transferrin - Selenium (ITS+1), 100 nM Dexamethasone, 10 ng/mL TGF- β, 50 µg/mL ascorbic acid, 40 µg/mL proline [45]) for 3 weeks. The medium was changed every 2-3 days.

4.4. Osteochondral collagen scaffold construction

A collagen gel was produced as described by the Invitrogen protocol provided with bovine collagen I [46]. Briefly, dH_2O, 10X Medium 199, 1N NaOH, and 5 mg/mL bovine collagen I, were mixed together in that order. Formulas provided in the Invitrogen protocol were used to determine the quantities of each component so that a firm collagen gel mixture with a pH of 7.0-7.5 could be produced [46]. hMSC derived osteoblasts were then trypsinized and counted with a hemocytometer. Trypsinized cells were centrifuged at 1250 RPM for 10 minutes to isolate a cell pellet. The pellet was then resuspended in the collagen gel mixture at $2.4*10^5$ cells/mL. 0.5 mL of cell-collagen gel mixture or collagen gel without cells was placed into each well of a 24-well plate already filled with chondrocyte beads (see section 4.3 above) to produce 9 replicates of each of the 5 groups outlined in Table 3.1 and Table 3.2. At this point each well contained $1.2*10^5$ osteoblasts and $1.2*10^5$ chondrocytes or only $2.4*10^5$ osteoblasts or only $2.4*10^5$ chondrocytes.

4.5. Cytokine Stimulation

After 3 days of culture in regular coculture medium, coculture medium supplemented with 50 pg/mL of IL-1β or 50 pg/mL of TNF-α was added to the appropriate experimental groups (see Table 3.1 and Table 3.2). These concentrations were determined by past studies showing that these concentrations were capable of inducing changes in gene expression consistent with osteoarthritis in chondrocytes [5]. Furthermore, the synovial fluid of patients with osteoarthritis has cytokine levels that fall within this range [15].

4.6. RNA extraction, reverse transcription and RT-PCR

Scaffolds were lysed with lysis buffer provided in a Qiagen RNeasy Mini Kit (Qiagen, Valencia, CA) and homogenized by passing through a 22-gauge needle repeatedly (≈10 times) [47]. After

homogenization, RNA was purified with the Quiagen RNeasy Mini Kit as described in the protocols provided with the kit [47].

RNA was then spectroscopically quantified with a nanodrop spectrometer (ND-3300, Nanodrop Technologies, USA). Using this quantification data, 50 ng of RNA from each sample was diluted to 50 µL in RNase free water. Then with a High-Capacity cDNA Archive Kit, (Applied Biosystems, Carlsbad, CA) reverse transcriptase master mix was prepared with the following components: nucleotide free water (21 µL/sample), 10x RT Buffer (10 µL/sample), 25x dNTPs (4 µL/sample), 10x random primers (10 µL/sample) and Multiscribe (5 µL/sample). The components were added in that order. Then, cDNA was reverse transcribed by adding 50 µL of reverse transcriptase master mix to the 50 µL of 50 ng RNA aliquoted before and running these samples through a thermocycler with the following program: 25° C for 10 minutes, 37°C for 120 minutes, 4 °C for 24 hours.

TaqMan Gene Expression assay-on-demand (AoD) kits (Applied Biosystems, Carlsbad, CA) and 2x TaqMan Universal PCR Mix (Applied Biosystems, Carlsbad, CA) were used to make a PCR master mix (17.5 µL/sample H_2O, 2.5 µL/sample AoD kit, 25 µL/sample Taqman Univ. PCR Kit). 45 µL of this PCR master mix was added to 5 µL of cDNA in a PCR plate for each sample and each gene. 3 biological and 2 technical replicates (total of 6 replicates) were run for each of the 5 experimental and control groups (see Table 3.1 and Table 3.2). Quantitative PCR was run on the plates using an Mx 3000 Real Time PCR system (Stratagene, CA). Transcriptional levels of the following TaqMan AoD genes were analyzed: ACAN, ADAMTS5, CASP3, MMP3, COL2A1, RUNX2, SOX9, and GAPDH. PCR statistical and data analysis was performed as described below in section 4.9.

4.7. Nitric Oxide Measurement

The Griess reagent kit (Molecular Probes, Eugene, OR) for nitrite determination was used to determine the nitric oxide content of supernatants from all groups collected 1 week and 2 weeks after cytokine stimulation. Manufacturer provided protocols were followed [48]. Briefly, 20 µL of Griess reagent was mixed with 150 µL of each sample and 130 µL of deionized water.

Serial dilution was employed to create 8 sodium nitrite standards ranging from 0-100 µM. The mixtures were incubated for 30 minutes at room temperature and absorbance was measured at 548 nm in a microplate reader (VERSAmax). Nitrite concentrations were determined by a standard curve (See Appendix 9.1). 3 biological replicates and 2 technical replicates of each group were used.

4.8. PicoGreen

A Quant-iT™ PicoGreen® dsDNA kit (Invitrogen, Carlsbad, CA) was used to quantify sample dsDNA. Scaffolds were lysed with 500 µL of lysis buffer (5 mM $MgCl_2$ solution with .2% (v/v) Triton X-100) and chopped to small bits with scissors. The scaffold/cell samples were centrifuged at 12000 rpm, 10 min, 4 °C and the DNA containing supernatant was collected and stored on ice. 75 µL of the collected supernatant from each sample was mixed with 25 µL of 1x TE Buffer in a 96 well plate. Standards were prepared by diluting the lambda DNA standard provided in the PicoGreen kit with 1x TE Buffer to make 7 standards with concentrations ranging from 0 ng/mL to 250 ng/mL. Each well was then loaded with 100 µL of Quant-iT PicoGreen dsDNA reagent provided in the kit. Plates were incubated at room temperature for 2-5 minutes and shaken for 60 seconds. Fluorescence was measured with an excitation wavelength of 480 nm and an emission wavelength of 520 nm in a microplate reader (VERSAmax). DNA concentrations were determined by a standard curve (See Appendix 9.2). 3 biological replicates and 2 technical replicates of each group were used.

4.9. Data analysis and Statistics

All quantitative data was measured using 3 biological replicates and 2 technical replicates (n=3) unless otherwise noted. Statistical significance was determined if $p<.05$ in any comparison of means. All error bars, as noted on the graphs, indicate +/- 2 standard errors (SE's).

For rtPCR analysis, first, any data point that did not have a C_t value was set to 51. The PCR machine was set to do 50 cycles and by assuming the next cycle (the 51st cycle) was the C_t point

for this null data, statistical analysis could be performed while minimizing any falsely significant statistical differences.

rtPCR data was analyzed using the $\Delta\Delta C_t$ method. Each data point was first normalized with GAPDH, an endogeneous reference gene, yielding $\Delta Ct = C_{t\ sample} - C_{t\ GAPDH}$. Each ΔC_t was then normalized again with the mean ΔC_t of all replicates of a control group yielding $\Delta\Delta C_t = \Delta C_{t\ sample} - \overline{\Delta C}_{t\ control}$, the $\Delta\Delta C_t$ of the control group was defined to be 0 since $\overline{\Delta C}_{t\ control} - \overline{\Delta C}_{t\ control} = 0$. Three different $\Delta\Delta C_t$'s were calculated for each replicate by normalizing with each of three different controls (osteochondral coculture, chondrocytes only, and osteoblasts only). For experimental and control group setup see Table 3.1 and Table 3.2.

Then, since PCR is an exponential growth process and C_t represents a linear cycle number, RQ, the relative quantity of each gene was calculated with the formula $RQ = 2^{-\Delta\Delta Ct}$. Note, that since the $\Delta\Delta C_t$ of the control group to which the rest of the data was normalized is defined to be 0, the RQ of the control group is defined to be 1 (2^0=1). A significant deviation above 1 then represents up-regulation of a gene relative to the control and a significant deviation below 1 represents down-regulation of a gene relative to the control.

Finally, the mean RQ of the 2 technical replicates for each of the 3 biological replicates was calculated and entered into SPSS (SPSS 19.0, Chicago, Illinois) to perform statistical analysis. Statistical significance was calculated on $\log_2$ transformed RQ data using a one-way ANOVA test as recommended by past studies on the statistical analysis of PCR [49]. Since ANOVA assumed equal variances, Levene's test was employed to test for homogeneity of variances and any test failing the homoscedasticity assumption was tested again with a non-parametric Kruskal-Wallis test. Then a post-hoc multiple comparison test was performed using Tukey's test. P values less than .05 were considered statistically significant.

Similarly, for PicoGreen and Nitrite assays after DNA concentrations and Nitrite concentrations of each replicate were calculated from the standard curve, the 2 technical replicates were averaged for each of the 3 biological replicates and ANOVA, Levene's test, and Tukey's post hoc multiple comparison test were employed to statistically analyze the data.

5. Results

5.1. ACAN RT-PCR Results

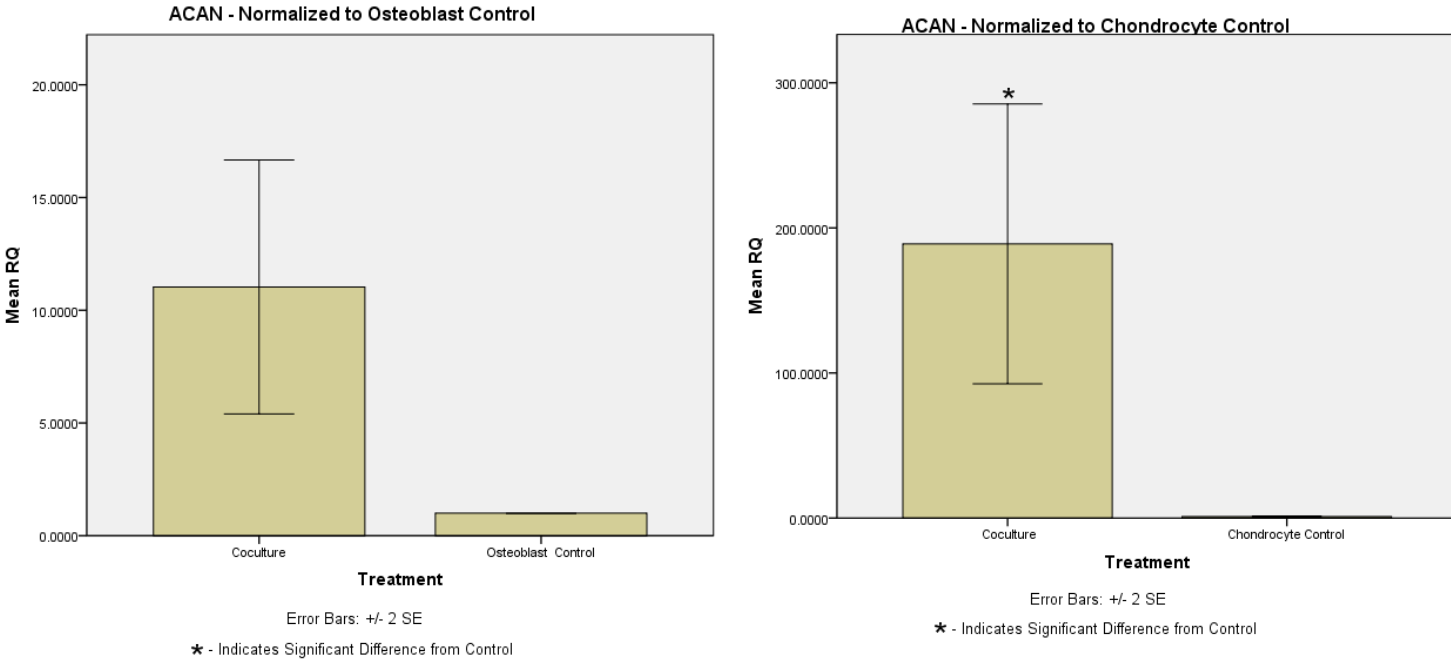

Figure 5.1 – Transcriptional levels of aggrecan in osteochondral coculture scaffolds normalized with osteoblast only scaffolds (on left) and chondrocyte only scaffolds (on right). Significance was determined at $p<.05$, $n=3$ unless otherwise specified.

Quantitative RT-PCR results showed that the untreated osteochondral coculture scaffolds showed significantly more aggrecan production than the chondrocyte only control scaffolds ($p<.0005$) as evidenced by the up-regulation of the ACAN gene. No significant differences were seen when compared with the osteoblast only control scaffold. In both cases there is a very large standard error (Figure 5.1).

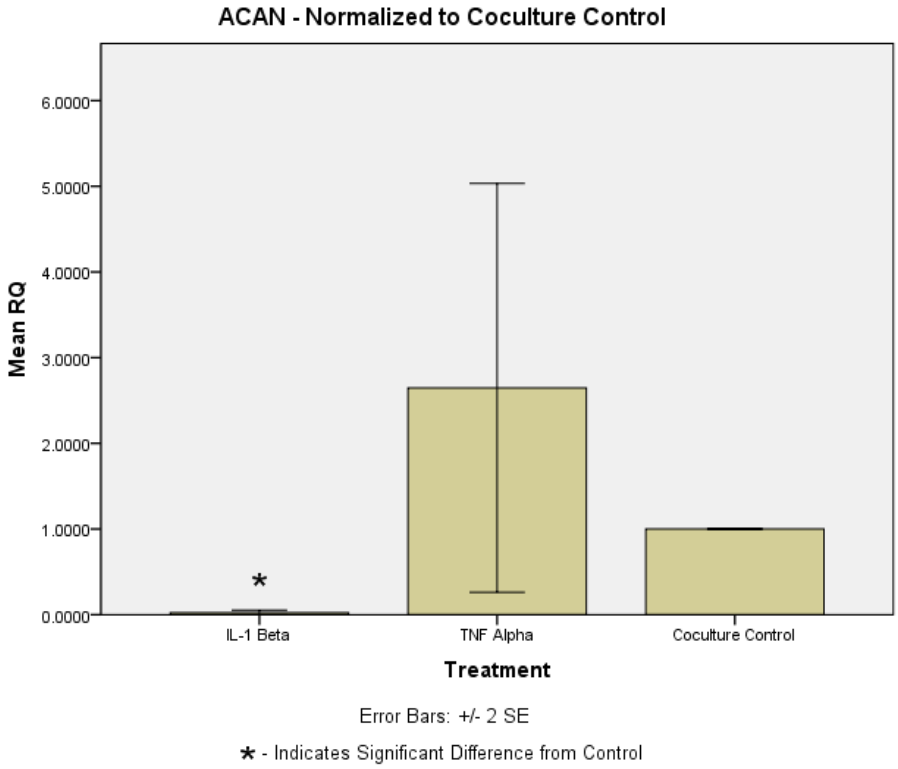

Figure 5.2 – Transcriptional levels of human aggrecan in osteochondral coculture under cytokine stimulated conditions (IL-1β and TNF-α) and un-stimulated conditions (coculture control). Data was normalized to coculture control and significance was determined at $p<.05$, $n=3$ unless otherwise specified.

Quantitative RT-PCR results showed that aggrecan synthesis was significantly down-regulated in IL-1β stimulated ($p=.04$) osteochondral cocultures compared to untreated, coculture controls. TNF-α stimulated osteochondral cocultures, however, showed no significant differences with the coculture control and a very large standard error (Figure 5.2).

5.2. ADAMTS5 PCR Results

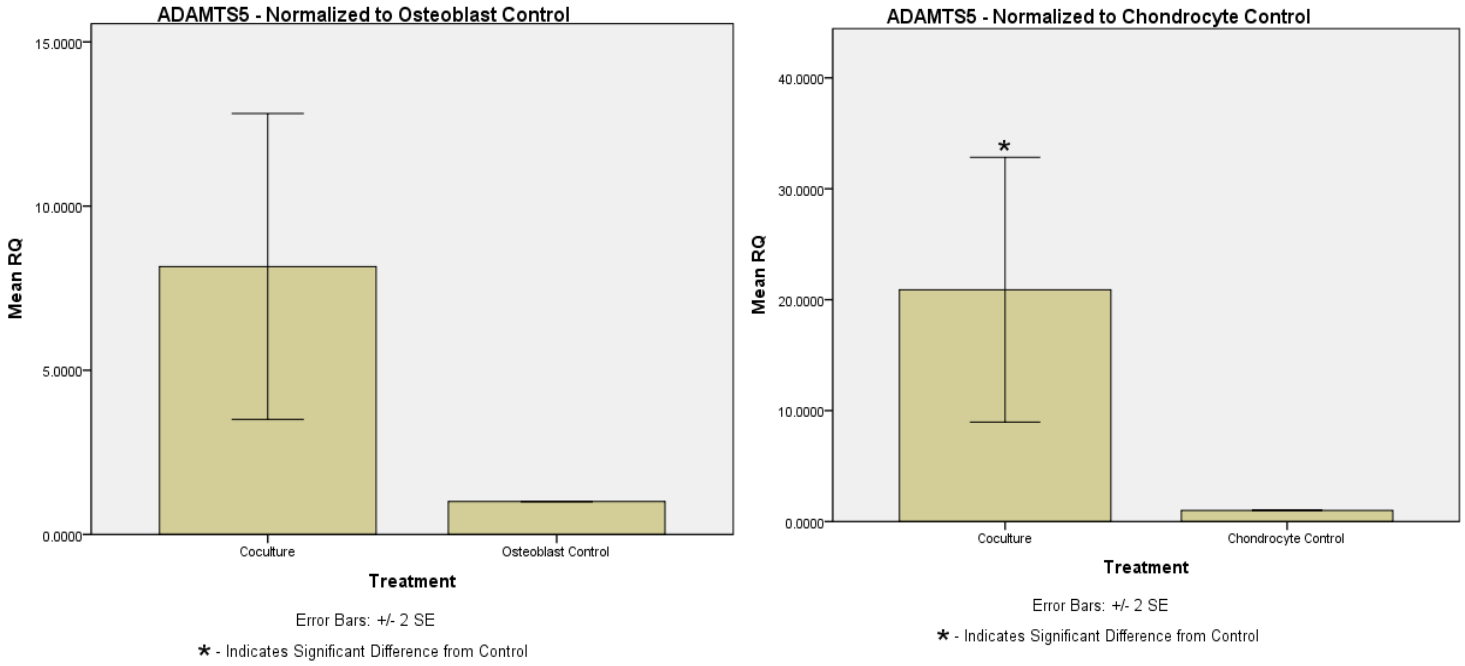

Figure 5.3 – Transcriptional levels of the aggrecanase, ADAMTS5 in osteochondral coculture scaffolds normalized with osteoblast only scaffolds (on left) and chondrocyte only scaffolds (on right). Significance was determined at $p<.05$, $n=3$ unless otherwise specified.

Quantitative RT-PCR results showed that un-stimulated osteochondral coculture scaffolds had significantly higher levels of ADAMTS5 (an aggrecanase gene) transcription than the chondrocyte only control scaffolds ($p=.003$), though there was a large standard error. No significant difference was seen between the untreated coculture scaffold and the osteoblast only control scaffold (Figure 5.3).

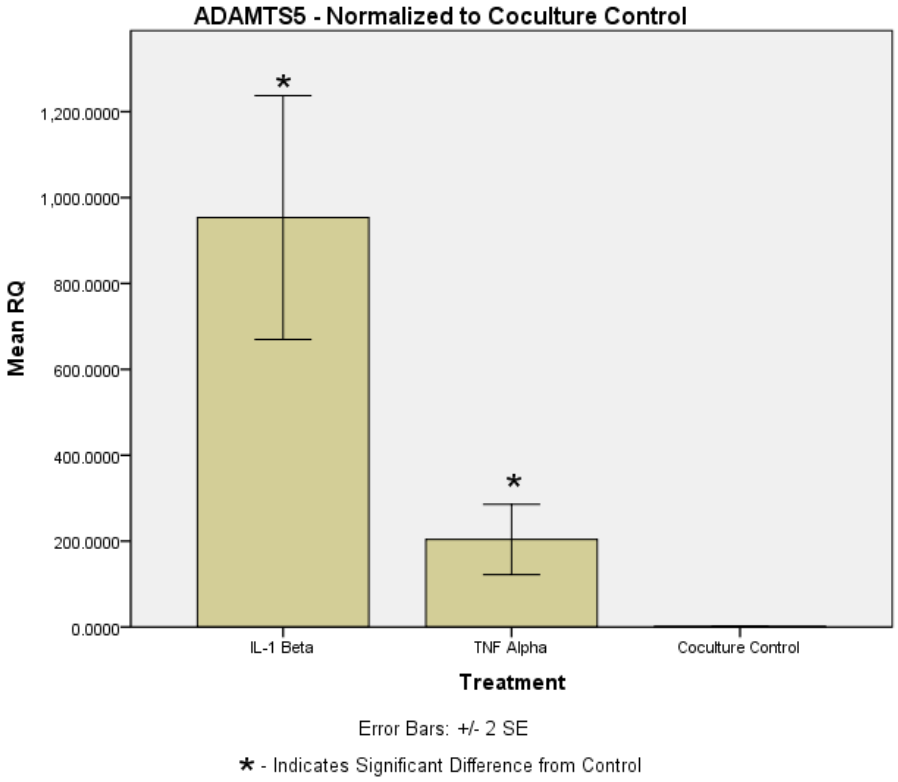

Figure 5.4 – Transcriptional levels of the aggrecanase, ADAMTS5 in osteochondral coculture under cytokine stimulated conditions (IL-1β and TNF-α) and un-stimulated conditions (coculture control). Data was normalized to coculture control and significance was determined at $p<.05$, $n=3$ unless otherwise specified.

Quantitative RT-PCR results showed that ADAMTS5 synthesis was significantly up-regulated in both IL-1β stimulated ($p<.0005$) and TNF-α stimulated ($p<.0005$) osteochondral coculture scaffolds when compared to untreated coculture scaffolds. IL-1β stimulated coculture scaffolds showed significantly more up-regulation compared to the coculture control than TNF- α (significance not shown on graph) (Figure 5.4).

5.3. MMP3 PCR Results

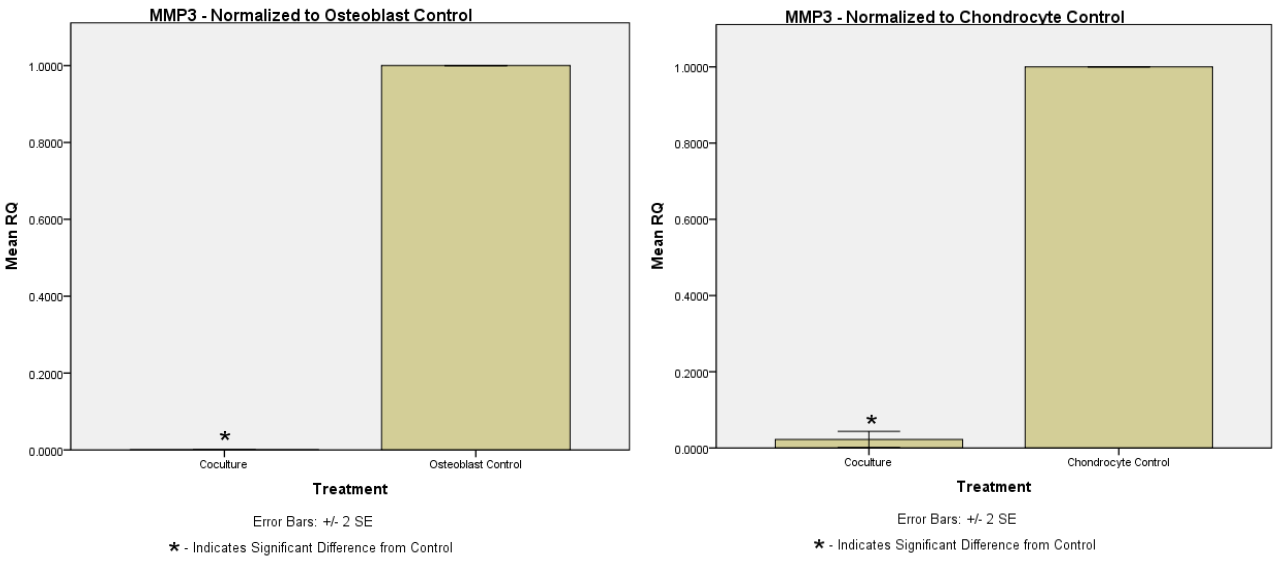

Figure 5.5 – Transcriptional levels of the metalloproteinase, MMP3 in osteochondral coculture scaffolds normalized with osteoblast only scaffolds (on left) and chondrocyte only scaffolds (on right). Significance was determined at $p<.05$, $n=3$ unless otherwise specified.

Quantitative RT-PCR results showed that un-stimulated osteochondral cocultures showed significantly less Matrix Metalloproteinase 3 (MMP3) transcription than both the chondrocyte only ($p=.002$) and osteoblast only control scaffolds ($p<.0005$) (Figure 5.5).

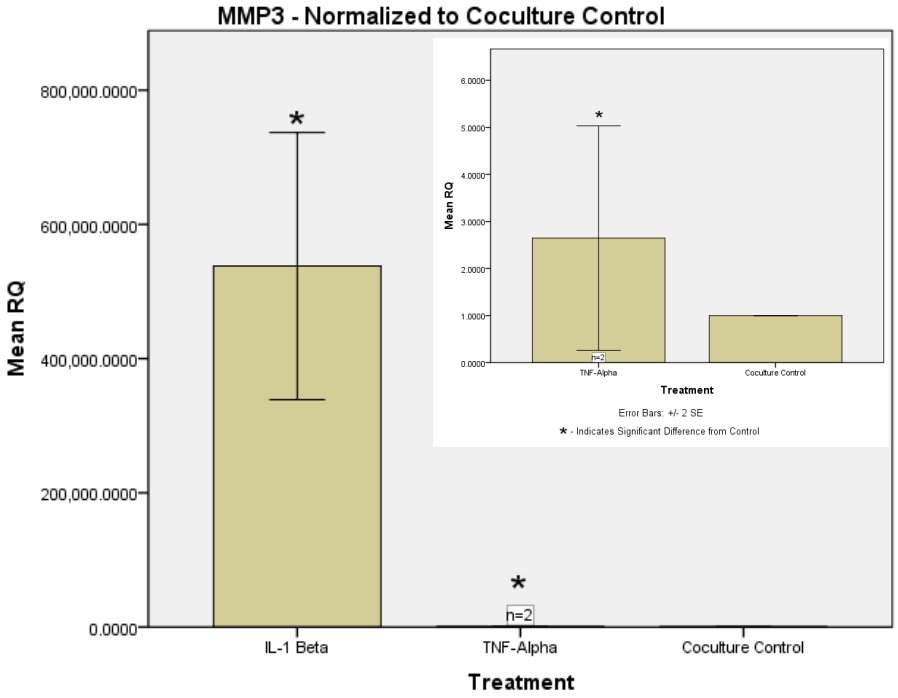

Figure 5.6 – Transcriptional levels of the metalloproteinase, MMP3 in osteochondral coculture under cytokine stimulated conditions (IL-1β and TNF-α) and un-stimulated conditions (coculture control). Data was normalized to coculture control and significance was determined at $p<.05$, n=3 unless otherwise specified

Quantitative RT-PCR results showed that MMP3 synthesis in osteochondral cocultures was significantly up-regulated under both IL-1β stimulation ($p<.0005$) and TNF-α stimulation ($p<.0005$) compared to un-stimulated coculture controls (Figure 5.6).

5.4. CASP3 PCR Results

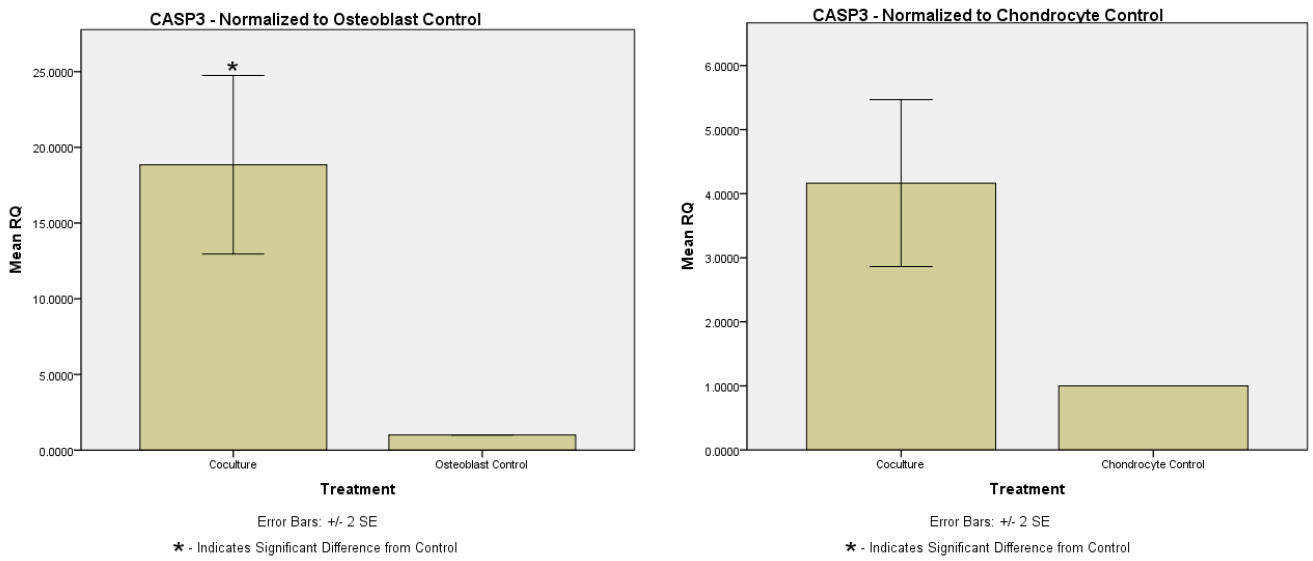

Figure 5.7 – Transcriptional levels of caspases 3 in osteochondral coculture scaffolds normalized with osteoblast only scaffolds (on left) and chondrocyte only scaffolds (on right). Significance was determined at $p<.05$, $n=3$ unless otherwise specified

Quantitative RT-PCR results showed that un-stimulated osteochondral cocultures showed significantly higher expressions of caspase 3 than the osteoblast only control scaffolds ($p=.014$) but no significant differences with chondrocyte only control scaffolds (Figure 5.7). In both cases there was a large standard error.

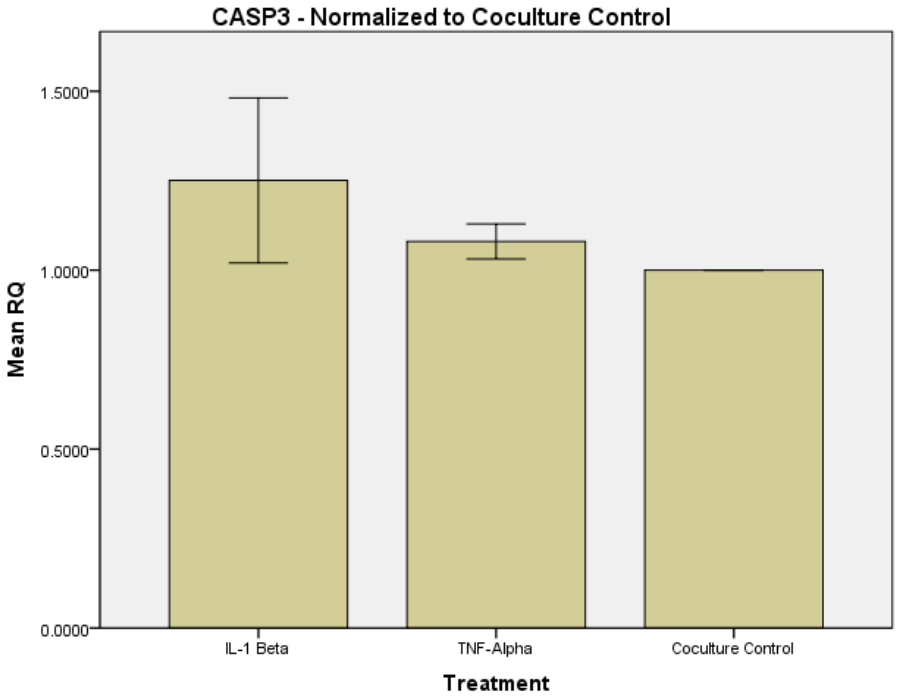

Figure 5.8 – Transcriptional levels of caspase 3 in osteochondral coculture under cytokine stimulated conditions (IL-1β and TNF-α) and un-stimulated conditions (coculture control). Data was normalized to coculture control and significance was determined at $p<.05$, $n=3$ unless otherwise specified.

Quantitative RT-PCR results showed that no significant differences were seen in caspase 3 expression between IL-1β stimulated osteochondral cocultures, TNF-α stimulated osteochondral cocultures and un-stimulated cocultures (Figure 5.8).

5.5. RUNX2 PCR Results

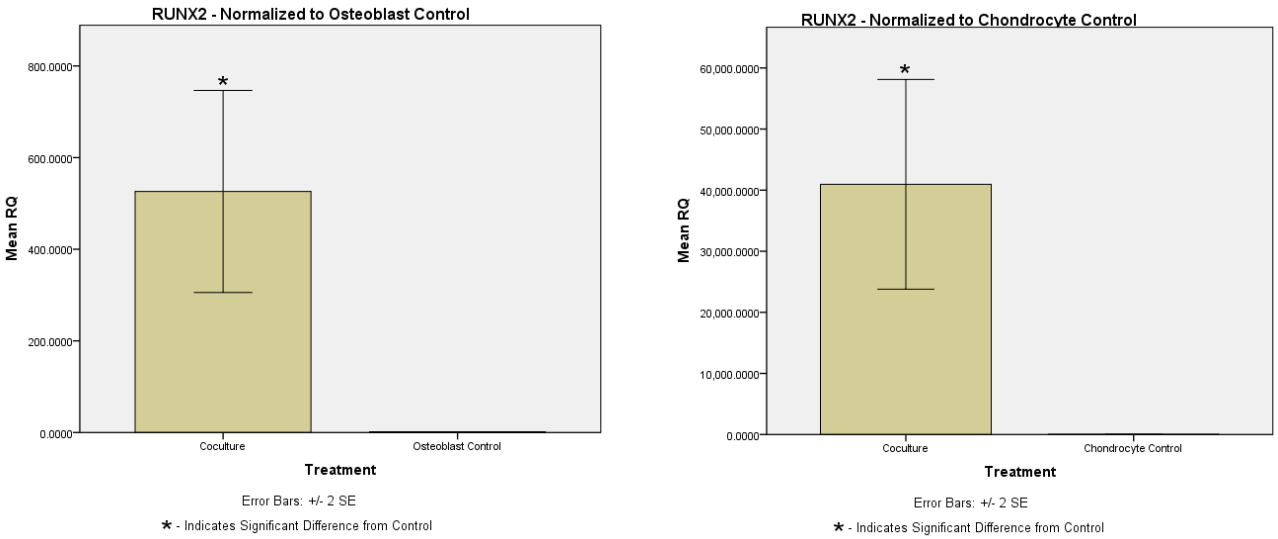

Figure 5.9 – Transcriptional levels of RUNX2 in osteochondral coculture scaffolds normalized with osteoblast only scaffolds (on left) and chondrocyte only scaffolds (on right). Significance was determined at $p<.05$, $n=3$ unless otherwise specified.

Quantitative RT-PCR results showed that un-stimulated cocultures showed significantly more RUNX2 transcription than both the chondrocyte only ($p<.0005$) and osteoblast only control scaffolds ($p<.0005$). Under both conditions, however, there is a large amount of standard error (Figure 5.9).

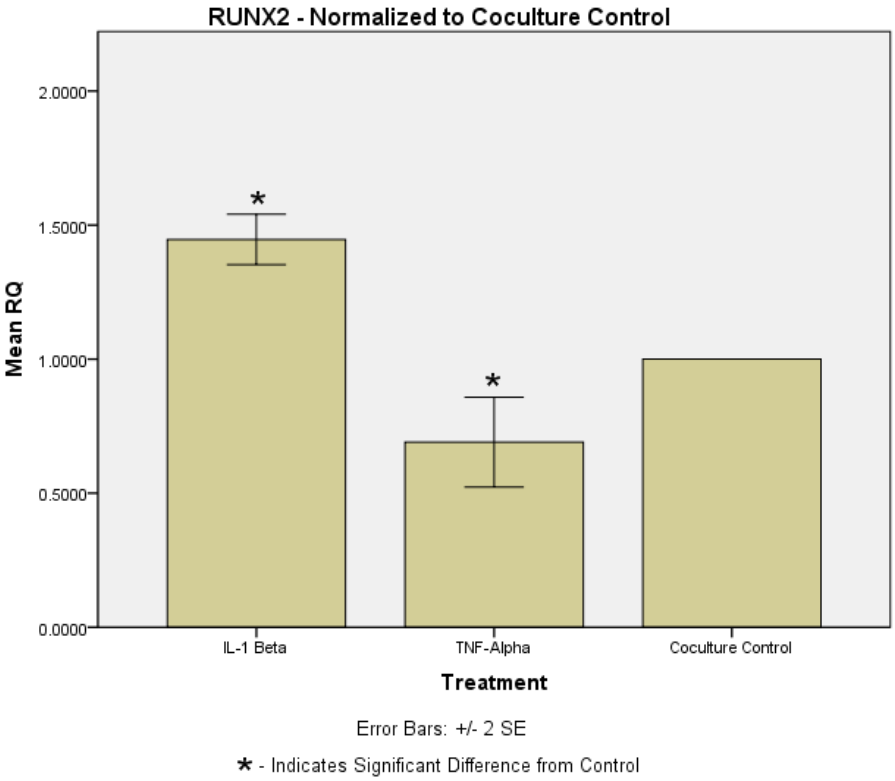

Figure 5.10 – Transcriptional levels of RUNX2 in osteochondral coculture under cytokine stimulated conditions (IL-1β and TNF-α) and un-stimulated conditions (coculture control). Data was normalized to coculture control and significance was determined at $p<.05$, $n=3$ unless otherwise specified.

Quantitative RT-PCR results showed that the osteoblast transcriptional factor, RUNX2, was significantly up-regulated in osteochondral cocultures under IL-1β stimulation ($p=.036$) and down-regulated under TNF-α stimulation ($p=.029$) (Figure 5.10) compared to un-stimulated cocultures.

5.6. SOX9 PCR Results

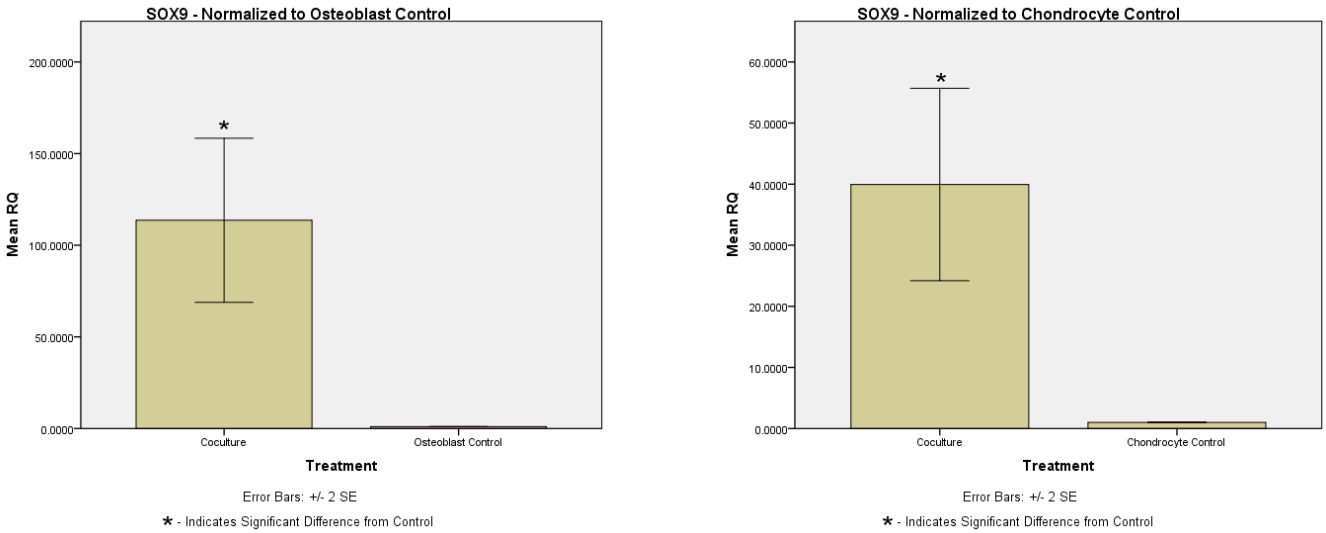

Figure 5.11 – Transcriptional levels of SOX9 in osteochondral coculture scaffolds normalized with osteoblast only scaffolds (on left) and chondrocyte only scaffolds (on right). Significance was determined at $p<.05$, $n=3$ unless otherwise specified.

Quantitative RT-PCR results showed that un-stimulated cocultures showed significantly more transcription of the chondrocyte differentiation factor, SOX9, than both the chondrocyte ($p<.0005$) and osteoblast controls ($p=.002$). Under both conditions, however, there is a large amount of standard error (Figure 5.11).

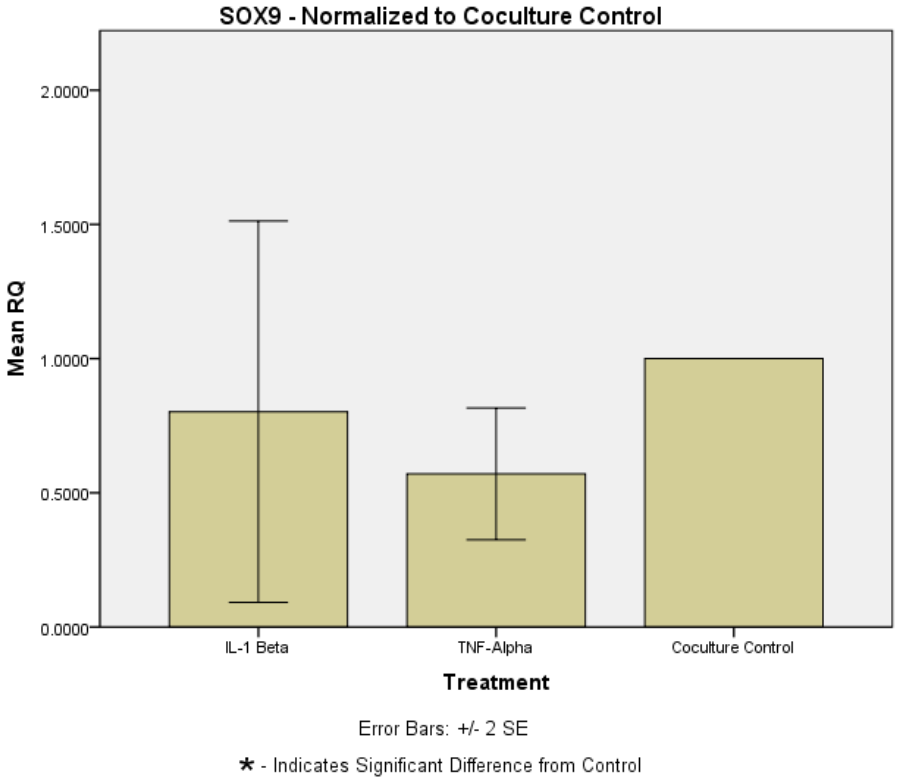

Figure 5.12 – Transcriptional levels of SOX9 in osteochondral coculture under cytokine stimulated conditions (IL-1β and TNF-α) and un-stimulated conditions (coculture control). Data was normalized to coculture control and significance was determined at $p<.05$, $n=3$ unless otherwise specified.

Quantitative RT-PCR results showed that no significant differences were seen in SOX9 transcription between IL-1β stimulated osteochondral cocultures, TNF-α stimulated osteochondral cocultures, and un-stimulated cocultures cocultures (Figure 5.12).

5.7. COL2A1 PCR Results

COL2A1 showed no detectable expression in any of the samples or groups. These anomalous results are discussed below in chapter 6 (Discussion).

5.8. Picogreen Results

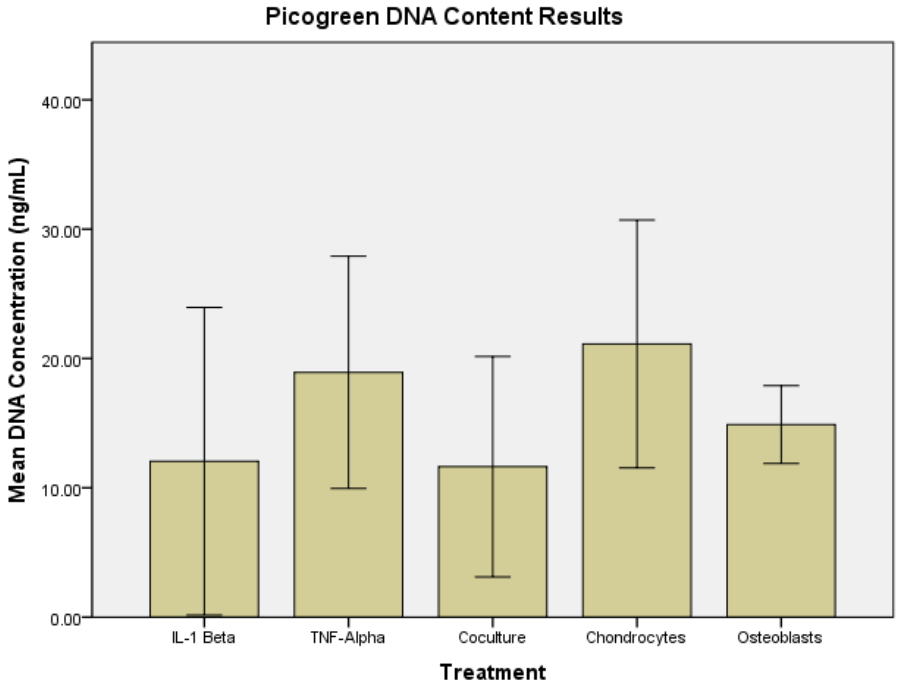

Figure 5.13 – Mean dsDNA concentration in cytokine stimulated osteochondral scaffolds (IL-1β and TNF-α), untreated coculture scaffolds, chondrocytes only, and osteoblast only scaffolds. Significance was determined at $p<.05$, n=3 unless otherwise specified.

PicoGreen analysis conducted 3 weeks after cytokine stimulation showed no significant differences in DNA concentration between any groups. Mean DNA quantities were small and ranged between 7-13 ng per sample (.67 mL of DNA solution per sample*DNA concentration from graph) (Figure 5.13).

5.9. Nitrite Assay Results

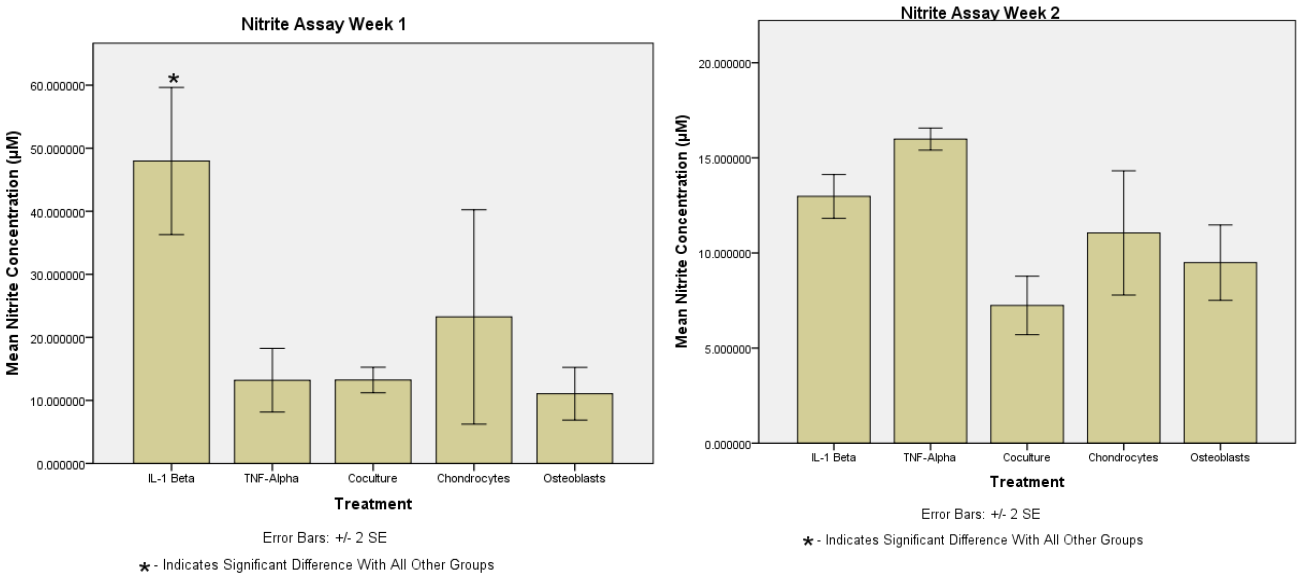

Figure 5.14 – Nitrite concentration in supernatant medium taken from cytokine stimulated osteochondral scaffolds (IL-1β and TNF-α), untreated coculture scaffolds, chondrocyte only, and osteoblast only scaffolds. Medium taken at week 1 is shown on the left and week is shown on the right. Significance was determined at $p<.05$, $n=3$ unless otherwise specified.

Nitrite assays showed significantly higher levels of nitrite in IL-1β stimulated osteochondral cocultures compared to all other groups after 1 week of cytokine stimulation ($p<.002$ for comparisons with all other groups). No significant differences in nitrite concentration were seen between any of the other groups after 1 week. No significant differences were seen between any groups after 2 weeks of cytokine stimulation (Figure 5.14).

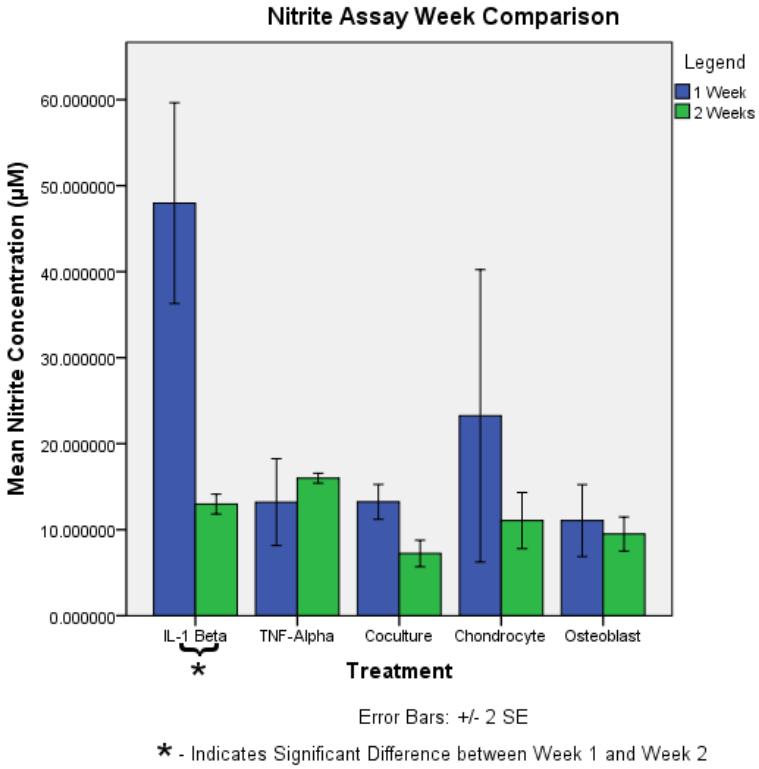

Figure 5.15 – Week by week comparison of nitrite concentration in supernatant medium taken from cytokine stimulated osteochondral scaffolds (IL-1β and TNF-α), untreated coculture scaffolds, chondrocyte only, and osteoblast only scaffolds. Significance was determined at $p<.05$, $n=3$ unless otherwise specified.

A week by week comparison of nitrite levels shows that a significant decrease in nitrite concentrations was seen between weeks 1 and 2 in IL-1β stimulated osteochondral cocultures ($p<.0005$) (Figure 5.15). No significant differences in nitrite concentrations were seen between weeks 1 and 2 for any of the other groups.

6. Discussion

6.1. Osteochondral Scaffold – Mechanical and cell population concerns

Osteochondral collagen scaffolds, qualitatively, showed weak mechanical properties. Scaffolds had fragile, soft structures very unlike the structure of native joints. Furthermore, the collagen gels shrunk after incubation yielding much smaller scaffolds than expected. The scaffolds also degraded quickly, becoming smaller over time. These mechanical properties can most likely be attributed to the collagen matrix. It may be possible to improve these properties by altering the collagen concentration and the pH of polymerization [50]. Alternatively, another biomaterial with better structural properties could be substituted or copolymerized with collagen. For instance, studies have shown that silk scaffolds cultured with MSC derived chondrocytes have structural properties resembling articular cartilage, which could make silk an ideal substitute for collagen in this study [51].

Another concern about the osteochondral coculture system is the low number of cells after prolonged culture. PicoGreen data from 3 weeks showed DNA content ranging from about 7-13 nanograms per sample. Assuming about 7 pg of dsDNA content in each human cell [52], this means the mean cell number per sample ranged from about 1000-2000 cells after 3 weeks. Considering that the samples were seeded with $2.4*10^5$ cells, this is a considerable reduction in cell number. This may have been caused by scaffold degradation over time. As mentioned previously, the scaffolds became appreciably smaller each day. Using a more stable biomaterial like silk may address this issue. Cell death could also be an indication of inadequate coculture media. To resolve this, different coculture medium formulations could be tested until cell survival rates increase.

6.2. Osteochondral Scaffold – Osteoblast and Chondrocyte Marker Expression

Osteoblast and chondrocyte gene markers showed ambiguous levels of expression relative to controls in osteochondral coculture scaffolds. Unexpectedly, a chondrocyte marker, aggrecan, was not significantly up-regulated compared to osteoblast only control scaffolds but was

significantly up-regulated compared to chondrocyte only control scaffolds giving no clear indication about the presence of chondrocytes in the osteochondral coculture (Figure 5.1). The chondrogenic transcriptional factor, RUNX2, showed up-regulation relative to both osteoblast and chondrocyte controls (Figure 5.9). Upregulation relative to osteoblast controls was expected, as chondrocyte markers should be up-regulated in chondrocytes compared to other cell types including osteoblasts. Upregulation relative to chondrocyte controls, however, was unexpected, as the chondrocyte control scaffold was seeded with twice the number of chondrocytes as the coculture scaffold so, if anything, there should have been down-regulation compared to the chondrocyte controls, not up-regulation. This could indicate the presence of chondrocytes in cocultures and possibly some interaction between osteoblasts and chondrocytes that results in increased levels of expression even relative to chondrocytes cultured alone. Another chondrocyte marker, COL2A1 showed no expression in any sample including the controls. This could possibly be caused by feedback inhibition of the collagen scaffold, though past studies have shown COL2A1 expression in collagen scaffolds so this is unlikely [53]. Another possibility is that the TaqMan probes used to quantify COL2A1 were defective or over saturated with light with previous use. It may be useful to run quantitative PCR again on COL2A1 with new TaqMan probes to confirm.

The osteogenic transcriptional factor, RUNX2, was up-regulated in osteochondral coculture scaffolds relative to both osteoblast only and chondrocyte only control scaffolds (Figure 5.11). This is the same behavior that was seen in the chondrogenic transcriptional factor, SOX9. Again, this could indicate the presence of osteoblasts in cocultures and some interaction between osteoblasts and chondrocytes that results in increased levels of expression even relative to osteoblasts cultured alone. The up-regulation of transcriptional factors might also indicate trans-differentiation between the three possible cell types in the final osteochondral construct: hMSC's, chondrocytes, and osteoblasts. This has been shown to occur in past studies [54].

6.3. Osteochondral Scaffold - Proteinase Expression

Interestingly, the matrix metalloproteinase, MMP3, was down-regulated in the osteochondral coculture compared to both osteoblast only and chondrocyte only control scaffolds (Figure 5.5). The aggrecanase, ADAMTS5, on the other hand was up-regulated in osteochondral cocultures compared to the chondrocyte control (Figure 5.3). MMP3 down-regulation could indicate remodeling and the construction of more ECM proteins upon coculturing. ADAMTS5 up-regulation relative to chondrocyte only control scaffolds but not osteoblast only control scaffolds might simply indicate that osteoblasts show elevated levels of ADAMTS5 compared to chondrocytes. The presence of osteoblasts in the coculture would then result in the up-regulation of ADAMTS5 in cocultures compared to chondrocyte controls that was seen.

6.4. Cytokine Stimulation – Protein and Proteoglycan Expression

As expected, aggrecan synthesis was significantly down-regulated upon IL-1β stimulation. As discussed previously (Section 2.1), this is expected in osteoarthritic tissue. TNF-α stimulation, on the other hand, did not show significant aggrecan down-regulation but this may be explained by TNF-α's lower potency [12, 15, 6] (Figure 5.2). A higher concentration of TNF-α should be tested to see if the same effects as IL-1β are elicited. The significant aggrecan down-regulation seen here suggests that cytokine stimulation is effective at inducing osteoarthritis like symptoms on these coculture scaffolds.

Since no COL2A1 expression was seen in any sample, nothing can be said about the effects of cytokine stimulation on collagen II expression.

6.5. Cytokine Stimulation – Proteinase and Nitric Oxide Expression

As expected, ADAMTS5 (aggrecanase gene) and MMP3 (metalloproteinase gene) both showed significant up-regulation after both IL-1β and TNF-α cytokine stimulation (Figure 5.4 and Figure 5.6). As discussed previously (Section 2.1), this is expected in osteoarthritis tissue. IL-1β stimulated samples also showed significantly greater up-regulation than TNF-α stimulated

samples (Figure 5.4 and Figure 5.6) (significance not shown on graphs), which is consistent with studies that have reported on TNF-α's lower potency [12, 15, 6].

After one week of culture, nitrite levels were significantly higher after IL-1β stimulation but not TNF-α stimulation (Figure 5.14), which again can be explained by TNF- α's lower potency. Interestingly, after 2 weeks of culture there was no longer a significant difference in nitrite levels between any groups (Figure 5.14) and in fact, nitrite levels decreased significantly from week one in the IL-1β stimulated cocultures (Figure 5.15). A decrease in nitrite levels over time might indicate that the effects of these cytokines is temporary or that additional factors are necessary to sustain nitric oxide production in osteoarthritic tissue. Testing gene expression at later time points as well, points might help to reveal some more of the long term effects of cytokine stimulation on these cocultures.

Proteinase and nitrite up-regulation is characteristic of osteoarthritic tissue [18, 12, 15] indicating that these cytokines are effective at inducing osteoarthritis like symptoms at least in the short term.

6.6. Cytokine Stimulation – Apoptosis

No significant differences were seen in caspase-3 expression between cytokine stimulated groups and control groups (Figure 5.8). Also, PicoGreen data showed no significant differences in DNA content between any groups, indicating no differences in cell numbers (Figure 5.13). The lack of caspase-3 up-regulation and hypocellularity indicates that apoptosis was not induced in the cytokine stimulated cocultures. It is likely that additional factors like macrophage stimulation are necessary to induce osteoarthritic apoptosis.

6.7. Cytokine Stimulation – Transcriptional Factors

Interestingly, the osteoblast transcriptional factor, RUNX2 was significantly up-regulated after IL-1β stimulation and down-regulated after TNF-α stimulation (Figure 5.10). Up-regulation of osteoblast transcription after IL-1β stimulation might suggest increased bone remodeling which has been seen to occur in osteoarthritic tissue [9]. The inhibition seen in RUNX2 synthesis by

TNF-α is also consistent with past studies that have shown RUNX2 down regulation by TNF-α [55].

7. Conclusion

The success of the osteochondral collagen-alginate bead scaffold is unclear. Its weak structural properties suggest that design improvements need to be made such as supplementation of the collagen matrix with silk. The low cell counts after prolonged culture and rapid degradation are concerning. Furthermore, gene expression analysis hinted at the presence of osteoblasts and chondrocytes but was largely ambiguous. Aggrecan, a chondrocyte marker, wasn't up-regulated relative to osteoblast controls but was up-regulated relative to chondrocyte controls. The other markers, RUNX2 (osteoblast marker) and SOX9 (chondrocyte marker) were up-regulated relative to both chondrocytes and osteoblasts. Collagen II showed no expression in any group. This unclear data does not definitively show the presence of chondrocytes and osteoblasts in the final coculture.

Osteoarthritis induction in this system by cytokines was for the most part, successful. IL-1β induced cocultures had significantly decreased levels of aggrecan, increased matrix metalloproteinase levels, increased aggrecanase levels, increased nitrite levels, and possibly increased bone remodeling (RUNX2 up-regulation) as expected for osteoarthritic tissue. Nitrite levels after two weeks of culture, however, were significantly reduced which might indicate that these effects are temporary but additional testing is necessary to confirm this. No significant differences were seen in caspase expression or cell number indicating that apoptosis was not occurring, contrary to what would be expected in osteoarthritic tissue. It is possible that additional factors are necessary to induce apoptosis. TNF-α showed a similar trend as IL-1β but with less pronounced differences. This was expected as past studies have reported that TNF-α is less potent than IL-1β.

As a realistic, in-vitro, osteoarthritis model, this system shows potential but needs to be modified to address some of the issues revealed in this study. A similar system with a different biomaterial, such as silk, may address many of these issues and result in a more successful model.

8. Future Directions

Future studies should try different forms of stimulation to induce osteoarthritis. For instance, past studies have reported that macrophages are another essential component in osteoarthritis pathology and important in cartilage degradation [4, 56]. Combination approaches using IL-1β, TNF-α, and macrophages may further improve the realism of the model.

Culturing the cells in a bioreactor to simulate mechanical stress is another logical step for this study. Mechanical stress on joints greatly increases the likelihood of developing osteoarthritis [1, 57] and is thus an essential component in a good osteoarthritis model.

Once this model has been further developed, a more extensive biochemical analysis should be conducted and compared with a biochemical analysis of osteoarthritic tissue. If successful, the living, in vitro model might provide researchers with more clues about the underlying causes behind this disease. Furthermore, therapeutic drugs could be tested and studied with this model in a more efficient and realistic way than existing models.

9. Appendix

9.1. Nitrite Assay Standard Curve

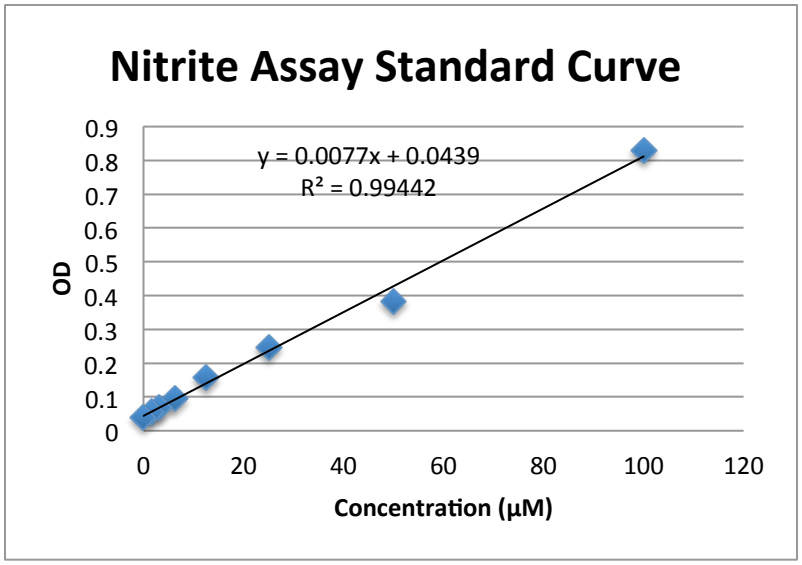

Figure 9.1 – Standard curve made to determine nitrite concentration using the Griess reagent. Standards were run in duplicate and averaged.

9.2. Picogreen Standard Curve

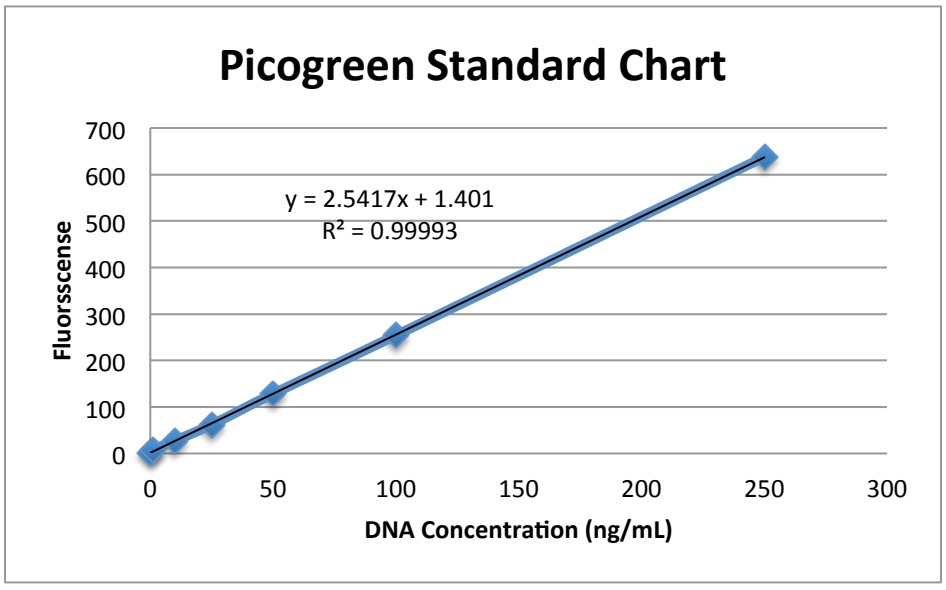

Figure 9.2 – Standard curve used to determine dsDNA concentration using PicoGreen. Standards were run in duplicate and averaged.

10. Works Cited

1. Conaghan P, Birrell F, Burke M, et al. Osteoarthritis National Clinical Guideline for Care and Management in Adults. *Royal College of Physicians*. 2008:4-29.
2. Pritzker KPH. Animal models for osteoarthritis: processes, problems and prospects. *Annals of the rheumatic Diseases*. 1994;53:406-419.
3. Goldring MB, Birkhead J, Sandell LJ, Kimura T, Krane SM. Interleukin 1 Suppresses Expression of Cartilage-specific Types 1 and IX Collagens and Increases Types I and III Collagens in Human Chondrocytes. *Journal of Clinical Investigation*. 1988;82:2026-2037.
4. Bondeson J, Wainwright SD, Lauder S, Amos N, Hughes CE. The role of synovial macrophages and macrophage-produced cytokines in driving aggrecanases, matrix metalloproteinases, and other destructive and inflammatory responses in osteoarthritis. *Arthritis Research & Therapy*. 2006;8(6):R187.
5. Richardson DW, Dodge GR. Effects of interleukin-1β and tumor necrosis factor-α on expression of matrix-related genes by cultured equine articular chondrocytes. *American Journal of Veterinary Research*. 2000;61(6):624-630.
6. Saklatvala J. Tumour necrosis factor alpha stimulates resorption and inhibits synthesis of proteoglycan in cartilage. *Nature*. 1986;322(7):547-549.
7. Articulation (Joint). *web-books*. 2011. Available at: http://www.web-books.com/eLibrary/Medicine/Physiology/Skeletal/Joint.htm. Accessed April 10, 2011.
8. Schuenke M, Schulte E, Schumacher U, Ross L. The Knee Koint: Capsule and Joint Cavity. In: Ross L, ed. *Thieme atlas of Anatomy*. New York: Thieme; 2006:400-401.
9. Karsdal MA, Leeming DJ, Bam EB, et al. Should subchondral bone turnover be targeted when treating osteoarthritis? *Osteoarthritis and Cartilage*. 2008;16:638-646.
10. Lajeunesse D, Reboul P. Subchondral bone in osteoarthritis: a biologic link with articular cartilage leading to abnormal remodeling. *Current Opinion in Rheumatology*. 2003;15:628-633.

11. Yang KGA, Saris DBF, Geuze RE, Rijen MH, Helm Y. Altered in vitro chondrogenic properties of chondrocytes harvested from unaffected cartilage in osteoarthritic joints. *Osteoarthritis and Cartilage*. 2006;14:561-570.
12. Goldring SR, Goldring MB. The role of cytokines in cartilage matrix degeneration in ostoarthritis. *Clinical Orthopaedics and Related Research*. Oct 2004(427S):S27-S36.
13. Goggs R, Carter SD, Schulze-Tanzil G, Shakibaei M, Mobasheri A. Apoptosis and the loss of chondrocyte survival signals contribute to articular cartilage degradation in osteoarthritis. *The Veterinary Journal*. 2003;166:140-158.
14. Goldring MB, Berenbaum F. The Regulation of Chondrocyte Function by Proinflammatory Mediators. *Clinical Orthopaedics and Related Research*. 2004;427S:S37-S46.
15. Westacott CI, Whicher JT, Barnes IC, Thompson D, Swan AJ, Dieppe PA. Synovial Fluid Concentration of Five Different Cytokines in Rheumatic Diseases. *Annals of Rheumatic Diseases*. 1990;49:676-681.
16. Karan A, Karan MA, Vural P, et al. Synovial fluid nitric oxide levels in patients with knee osteoarthritis. *Clinical Rheumatology*. 2003;22:397-399.
17. Scher JU, Pillinger MH, Abramson SB. Nitric oxide synthases and osteoarthritis. *Current Rheumatology Reports*. April 2007;9(1):9-15.
18. Karan A, Karan MA, Vural P, et al. Synovial fluid nitric oxide levels in patients with knee osteoarthritis. *Clinical Rheumatology*. 2003;22:397-399.
19. The Abramson Lab. Osteoarthritis Research. *NYU School of Medicine*. 2007. Available at: http://www.med.nyu.edu/medicine/labs/abramsonlab/osteoarth-research.html. Accessed May 16, 2011.
20. Maneiro E, Lopez-Armada MJ, de Andres MC, et al. Effect of nitric oxide on mitochondrial respiratory activity of human articular chondrocytes. *Annals of Rheumatic Disease*. 2005;64:388-395.

21. Burr DB, Radin EL. Microfractures and microcracks in subchondral bone: are they relevant to osteoarthritis. *Rheumatic Disease Clinics of North America*. 2003;29:675-685.
22. Ameye LG, Young MF. Animal models of osteoarthritis: lessons learned while seeking the 'Holy Grail. *Current Opinion in Rheumatology*. 2006;18(5):537-547.
23. Huser CAM, Davies EM. Validation of an In Vitro Single-Impact Load Model of the Initiation of Osteoarthritis-like Changes in Articular Cartilage. *Journal of orthopaedic research*. 2006;24(4):725-732.
24. Thompson RC, Oegema TR. Metabolic activity of articular cartilage in osteoarthritis. An in vitro study. *The Journal of Bone and Joint Surgery*. 1979;61-A(3):407-416.
25. Verner MJ, Thompson RC, Lewis JK, Oegema TR. Subchondral Damage After Acute Transarticular Loading: An In Vitro Model of Joint Injury. *Orthopaedic Research Society*. 1992;10:759-765.
26. Cao T, Ho K, Teoh S. Scaffold Design and in Vitro Study of Osteochondral Coculture in a Three-Dimensional Porous Polycaprolactone Scaffold Fabricated by Fused Deposition Modeling. *Tissue Engineering*. 2003;9:103-111.
27. Invitrogen Corporation. Collagenase Type 1. *Invitrogen*. June 2004. http://products.invitrogen.com/ivgn/product/17100017. Accessed April 12, 2011.
28. Serp D, Cantana E, Heinzen C, von Stocker U, Marison IW. Characterization of an Encapsulation Device for the Production of Monodisperse Alginate Beads for Cell Immobilization. *Biotechnology and Bioengineering*. 2000;70(1):41-53.
29. Ignatius A, Blessing H, Liedert A, et al. Tissue engineering of bone: effects of mechanical strain on osteoblastic cells in type I collagen matrices. *Biomaterials*. 2005;26:311-318.
30. Casser-Bette M, Murray AB, Closs EI, Erfle V, Schmidt J. Bone formation by osteoblast-like cells in a three-dimensional cell culture. *Calcified Tissue International*. 1990;46(1):46-56.
31. Kinoshita S, Finnegan M, Bucholz RW, Mizuno K. Three-dimensional collagen gel culture promotes osteoblastic phenotype in bone marrow derived cells. *International Journal of Medical Sciences*. 1999;45(5):201-211.

32. Masi L, Franchi A, Santucci M, et al. Adhesion, growth, and matrix production by osteoblasts on collagen substrata. *Calcified Tissue International*. 1992;51(3):202-212.

33. De Ceuninck F, Lesure C, Pastoureau P, Caliez A, Sabatini M. Culture of Chondrocytes in Alginate Beads. *Methods in Molecular Medicine*. 2004;100:15-22.

34. Xu J, Wang W, Ludeman M, et al. Chondrogenic Differentiation of Human Mesenchymal Stem Cells in Three-Dimensional Alginate Gels. *Tissue Engineering*;14(5):667-680.

35. Beyer NN, da Silva ML. Mesenchymal Stem Cells: Isolation, In Vitro Expansion and Characterization. In: Wobus AM, Boheler K, eds. *Stem Cells*. Vol 174. 1st ed: Springer; 2008:249-282.

36. Sive JI, Baird P, Jeziorsk M, Watkins A, Hoyland JA, Freemont AJ. Expression of chondrocyte markers by cells of normal and degenerate intervertebral discs. *Journal of Clinical Pathology*. 2002;55:91-91.

37. Bau B, Gebhard PM, Haag J, Knorr T, Bartnik E, Aigner T. Relative Messenger RNA Expression Profiling of Collagenases and Aggrecanases in Human Articular Chondrocytes In Vivo and In Vitro. *Arthritis & Rheumatism*. 2002;46(10):2648-2657.

38. Tortorella MD, Malfair AM, Deccico C, Amer E. The role of ADAM-TS4 (aggrecanase-1) and ADAM-TS5 (aggrecanase-2) in a model of cartilage degradation. *Journal of OsteoArthritis Research Society International*. 2001;9:539-552.

39. Franceschi RT, Xiao G, Jiang D, Gopalakrishnan R, Yang S, Reith E. Multiple Signaling Pathways Converge on the Cbfa1/Runx2 Transcription Factor to Regulate Osteoblast Differentiation. *Connective Tissue Research*. 2003;44(Suppl. 1):109-116.

40. Sun H, Ye F, Wang J, et al. The Upregulation of Osteoblast Marker Genes in Mesenchymal Stem Cells Prove the Osteoinductivity of Hydroxyapatite/Tricalcium Phosphate Biomaterial. *Transplantaion Proceedings*. 2008;40:2645-2648.

41. Hadkidakis DJ, Androulakis II. Bone Remodeling. *Annals of the New York Academy of Sciences*. 2007;1092(1):385-396.

42. Furumatsu T, Asahara H. Histone Acetylation Influences the Activity of Sox9-related Transcriptional Complex. *Acta Medica Okayama*. 2010;64(6):351-357.

43. Jalswal N, Haynesworth SE, Caplan AI, Bruder SP. Osteogenic Differentiation of Purified, Culture-Expanded Human Mesenchymal Stem Cells In Vitro. *Journal of Cellular Biochemistry*. 1997;64:295-312.

44. Lonza Walkersville, Inc. Clonetics® Normal Human Articular Chondrocytes (NHAC-kn)

45. Mackay AM, Beck SC, Murphy JM, Barry FP, Chichester CO, Pittenger MF. Chondrogenic Differentiation of Cultured Human Mesenchymal Stem Cells from Marrow. *Tissue Engineering*. 1998;4(4):415-428.

46. Invitrogen Corporation. Collagen I, Bovine

47. Quiagen. RNeasy Mini Handbook

48. Molecular Probes. Griess Reagent Kit for Nitrite Determination (G-7921)

49. Yuan JS, Reed A, Chen F, Stewart NC. Statistical analysis of real-time PCR data. *BMC Bioinformatics*. 2006;7(85):1-12.

50. Roeder BA, Kokini K, Sturgis JE, Robinson JP, Voytik-Harbin SL. Tensile Mechanical Properties of Three-Dimensional Type I Collagen Extracellular Matrices With Varied Microstructure. *Journal of Biomechanical Engineering*. April 2002;124(2):214-222.

51. Wang Y, Kim UJ, Blasioli Dj, Hyeon-Joo K, Kaplan DL. In vitro cartilage tissue engineering with 3D porous aqueous-derived silk scaffolds and mesenchymal stem cells. *Biomaterials*. 2005;26:7082-7094.

52. Otto WR. Fluorimetric DNA Assay of Cell Number. *Methods in Molecular Biology*. 2005;289:251-262.

53. Mukaida T, Urabe K, Naruse K, et al. Influence of three-dimensional culture in a type II collagen sponge on primary cultured and dedifferentiated chondrocytes. *Journal of Orthopaedic Science*. 2005;10:521-528.

54. Song L, Tuan RS. Transdifferentiation potential of human mesenchymal stem cells derived from bone marrow. *The FASEB Journal*. 2004;18:980-982.

55. Gilbert L, He X, Farmer P, et al. Expression of the Osteoblast Differentiation Factor RUNX2 (Cbfa1/ AML3/Pebp2 alpha A) Is Inhibited by Tumor Necrosis Factor- alpha. *The Journal of Biological Chemistry*. 2002;277(4):2695-2701.

56. Janusz MJ, Hare M. Cartilage degradation by cocultures of transformed macrophage and fibroblast cell lines. A model of metalloproteinase-mediated connective tissue degradation. *Journal of Immunology*. 1993;150:1922-1931.

57. Obeid EM, Adams MA, Newman JH. Mechanical Properties of Articular Cartilage in Knees with Unicompartmental Osteoarthritis. *British Editorial Society of Bone and Joint Surgery*. 1994;76-B(2):315-319.